

Oxygen abundances in planet-harbouring stars. *

Comparison of different abundance indicators.

A. Ecuvillon¹, G. Israelian¹, N. C. Santos^{2,3}, N. G. Shchukina⁴, M. Mayor³ and R. Rebolo^{1,5}

¹ Instituto de Astrofísica de Canarias, E-38200 La Laguna, Tenerife, Spain

² Centro de Astronomia e Astrofísica de Universidade de Lisboa, Observatorio Astronomico de Lisboa, Tapada de Ajuda, 1349-018 Lisboa, Portugal

³ Observatoire de Genève, 51 ch. des Maillettes, CH-1290 Sauverny, Switzerland

⁴ Main Astronomical Observatory, National Academy of Sciences, 27 Zabolotnogo Street, 03680 Kyiv-127, Ukraine

⁵ Consejo Superior de Investigaciones Científicas, Spain

Received 19 May 2005 / Accepted 16 August 2005

Abstract. We present a detailed and uniform study of oxygen abundances in 155 solar type stars, 96 of which are planet hosts and 59 of which form part of a volume-limited comparison sample with no known planets. EW measurements were carried out for the [O I] 6300 Å line and the OI triplet, and spectral synthesis was performed for several OH lines. NLTE corrections were calculated and applied to the LTE abundance results derived from the O I 7771–5 Å triplet. Abundances from [O I], the O I triplet and near-UV OH were obtained in 103, 87 and 77 dwarfs, respectively. We present the first detailed and uniform comparison of these three oxygen indicators in a large sample of solar-type stars. There is good agreement between the [O/H] ratios from forbidden and OH lines, while the NLTE triplet shows a systematically lower abundance. We found that discrepancies between OH, [O I] and the O I triplet do not exceed 0.2 dex in most cases. We have studied abundance trends in planet host and comparison sample stars, and no obvious anomalies related to the presence of planets have been detected. All three indicators show that, on average, [O/Fe] decreases with [Fe/H] in the metallicity range $-0.8 < [\text{Fe}/\text{H}] < 0.5$. The planet host stars present an average oxygen overabundance of 0.1–0.2 dex with respect to the comparison sample.

Key words. stars: abundances – stars: chemically peculiar – stars: evolution – stars: planetary systems – Galaxy: solar neighbourhood

1. Introduction

The discoveries of more than 120 planetary-mass companions orbiting around solar-type stars have provided important opportunities to understand the formation and evolution of planetary systems. Several studies have shown that planet-harbouring stars are on average more metal-rich than dwarfs of the same spectral type with no known planets (Gonzalez 1997; Gonzalez et al. 2001; Laws et al. 2003; Santos et al. 2001, 2003b, 2004a, 2005; for a review see Santos et al. 2003a). Two possible explanations have been suggested to link the metallicity excess

to the presence of planets. The first has been proposed by Gonzalez (1997), who has suggested that the iron enhancement observed in stars with planets is due mainly to the accretion of large amounts of protoplanetary material onto the star. The other hypothesis by Santos et al. (2000, 2001) attributes the metallicity excess of planet host stars to the high metal content of the primordial cloud out of which the planetary system formed.

Detailed chemical analysis of planet-harbouring stars can provide useful information in the understanding of how the systems with giant planets have formed. Searching for chemical anomalies related to the presence of planets, in addition to the observed iron excess, is thus of high interest in discriminating between possible planetary formation hypotheses. For instance, light elements can give important evidence of pollution events (Israelian et al. 2001b, 2003a, 2004a; Sandquist et al. 2002; Santos et al. 2002, 2004b).

Abundance trends of volatile and refractory elements are also of interest in investigating planetary system formation. If the accretion processes were mainly responsible for the metallicity excess found in planet host stars, a relative overabun-

Send offprint requests to: e-mail: aecuvill@ll.iac.es

* Based on data from the FEROS spectrograph at the 2.2-m ESO/MPI telescope (observing run ID 074.C-0135), at the La Silla Observatory, ESO (Chile), and the UVES spectrograph at VLT/UT2 Kueyen telescope (observing run ID 074.C-0134), at the Paranal Observatory, ESO (Chile), and on observations made with the SARG spectrograph at 3.5-m TNG, operated by the Fundación Galileo Galilei of the INAF, and with the UES spectrograph at the 4-m William Hershel Telescope (WHT), operated by the Isaac Newton Group, both at the Spanish Observatorio del Roque de los Muchachos of the Instituto de Astrofísica de Canarias.

dance of refractory elements would be observed, since volatiles (with low condensation temperatures) are expected to be deficient in accreted materials (Smith et al. 2001). Likewise, if planet host stars had undergone significant pollution, their volatile abundances should show clear differences with respect to those of field stars. In this framework, it is very important to achieve abundance trends for as many planet host stars and as many elements as possible, and to carry out a homogeneous comparison with field stars with no known planetary-mass companion.

Several studies on abundances of metals other than iron have been carried out in planet host stars, but most of them have included only a reduced number of targets with planets and their results have been compared inhomogeneously with abundance trends of field stars from other authors (Gonzalez & Laws 2000; Gonzalez et al. 2001; Santos et al. 2000; Takeda et al. 2001; Sadakane et al. 2002; for a review see Israelian et al. 2003b). Recently, some refractories (e.g. Ca, Ti, Si, etc.) and volatiles (N, C, S and Zn) have been analysed homogeneously in a large number of planet host targets, as well as in a comparison set of stars with no known planets (Bodaghee et al. 2003; Ecuvillon et al. 2004a, 2004b; Beirao et al. 2005; Gilli et al. 2005). Takeda & Honda (2005) presented a study of CNO abundances in 27 planet host stars included in a large sample of 160 F, G and K dwarfs and subgiants.

Oxygen is the third most abundant element in the Universe, after hydrogen and helium. By analysing elemental abundances in the atmospheres of F and G dwarfs stars it is possible to determine the chemical composition of the gas out of which the stars were born and to understand the chemical evolution of the Galaxy and its formation history (e.g. McWilliam 1997). Oxygen is essentially primary. It is formed by α -processing in massive stars and released in the interstellar medium (ISM) during Type II SN explosions (e.g. Arnett 1978; Tinsley 1979; Woosley & Weaver 1995).

Several indicators have been used in the determination of oxygen abundances in disc and halo stars: the near-IR OI triplet at 7771–5 Å (e.g. Abia & Rebolo 1989; Tomkin et al. 1992; King & Boesgaard 1995; Cavallo, Pilachowski, & Rebolo 1997; Mishenina et al. 2000; Israelian et al. 2001a; Fulbright & Johnson 2003; Takeda 2003; Bensby, Feltzing, & Lundström 2004; Schukina et al. 2005), the forbidden lines of [OI] at 6300 and 6363 Å (e.g. King & Boesgaard 1995; Fulbright & Johnson 2003; Takeda 2003; Bensby, Feltzing, & Lundström 2004; Schukina et al. 2005), and the near-UV OH lines at 3100 Å (e.g. Bessell, Sutherland, & Ruan 1991; Nissen et al. 1994; Israelian, García-López, & Rebolo 1998; Boesgaard et al. 1999; Israelian et al. 2001a). Unfortunately, results from different indicators show discrepancies. Israelian et al. (2004b) have reported the largest conflict between the OI triplet at 7771–5 Å and the forbidden line at 6300 Å with discrepancies in [O/H] ratios of up to 1 dex. For stars with $[Fe/H] < -1.0$, many studies obtained disagreement in the [O/Fe] vs. [Fe/H] relationship (e.g. Israelian et al. 2001a; Nissen et al. 2002). For solar-metallicity stars as well the situation is unclear (e.g. Nissen & Edvardsson 1992; Feltzing & Gustafsson 1998; Prochaska et al. 2000; Bensby, Feltzing, & Lundström 2004).

The analyses of these lines all have their difficulties. The triplet lines are strongly affected by deviations from LTE (e.g. Shchukina 1987; Kiselman 1991), and by convective inhomogeneities (e.g. Kiselman 1993). However newer 3D calculations by Asplund et al. (2004) showed that the NLTE effects are very similar in 1D and 3D. The forbidden lines are both very weak and blended by lines from other species (e.g. Lambert 1978; Bensby, Feltzing, & Lundström 2004). The OH lines are very sensitive to surface inhomogeneities like granulation (e.g. Kiselman & Nordlund 1995).

Our work presents a complete and uniform study of the oxygen abundances in two large samples, a set of planet-harbouring stars and a volume-limited comparison sample of stars with no known planetary-mass companions, using three different indicators in order to check the consistency of the results. We carry out a detailed comparison among the abundances provided by different lines and discuss possible discrepancies. We investigate eventual anomalies related to the presence of planets and locate our results within the framework of Galactic chemical evolution.

2. Observations

Most of the spectra for the [OI] line and OI triplet analysis were collected during several observational campaigns with different spectrographs: CORALIE on the 1.2 m Euler Swiss telescope, FEROS on the 2.2 m ESO/MPI telescope (both at La Silla, Chile), UVES at the VLT/UT2 Kueyen telescope (Paranal, ESO, Chile), SARG on the 3.5 m TNG and UES on the 4.2 m WHT (both at Roque de los Muchachos, La Palma, Spain). Previous works have already used them to derive stellar parameters (Santos et al. 2004a) and abundances of different species (Bodaghee et al. 2003; Ecuvillon et al. 2004a, 2004b; Beirao et al. 2005; Gilli et al. 2005).

New optical spectra were collected with the UVES spectrograph at the Kueyen telescope, the FEROS spectrograph at the ESO/MPI telescope and the SARG spectrograph at TNG (Roque de los Muchachos, La Palma, Spain). A detailed description of the FEROS data is available in the work of Santos et al. (2005). The new optical SARG and UVES spectra have a resolution $R \sim 57\,000$ and $R \sim 85\,000$, as well as S/N ratios above 150 and 600, respectively, at ~ 6000 Å.

For the synthesis of the OH lines, we used the near-UV spectra from the UVES spectrograph at the Kueyen telescope, from which Santos et al. (2002) and Ecuvillon et al. (2004a) have derived beryllium and nitrogen abundances. We refer the reader to these papers for a detailed description of the data. New near-UV spectra obtained from the UVES spectrograph at the Kueyen telescope were used. These spectra have a resolution $R \sim 75\,000$ and S/N ratios above 100 in most cases at Be region.

The data reduction for the new SARG spectra was done using IRAF¹ tools in the echelle package. Standard background

¹ IRAF is distributed by the National Optical Astronomy Observatories, operated by the Association of Universities for Research in Astronomy, Inc., under cooperative agreement with the National Science Foundation, USA.

Table 1. Atomic parameters adopted for [OI] 6300 Å line, OI 7771–5 Å triplet and the near-UV OH lines.

Species	λ (Å)	χ_I (eV)	$\log gf$
[OI]	6300.230	0.00	-9.689
Ni I	6300.399	4.27	-2.310
O I	7771.960	9.11	0.452
O I	7774.180	9.11	0.314
O I	7775.400	9.11	0.099
OH	3167.169	1.11	-1.623
OH	3189.312	1.03	-1.990
OH	3255.490	1.30	-1.940
OH	3172.997	1.20	-1.692
OH	3173.200	1.83	-1.100

correction, flatfield and extraction procedures were used. The wavelength calibration was performed using a ThAr lamp spectrum taken during the same night. The FEROS and UVES spectra were reduced using the corresponding pipeline softwares.

3. Analysis

Abundance ratios were derived from three different indicators: the forbidden line at 6300 Å, the OI 7771–5 Å triplet, and a set of five near-UV OH lines at 3100 Å. *EW* measurements were carried out for the [OI] line and the triplet, while spectral synthesis was performed for the OH lines.

LTE abundances for all the indicators were determined according to a standard analysis with the revised version of the spectral synthesis code MOOG² (Sneden 1973) and a grid of Kurucz (1993) ATLAS9 atmospheres with overshooting (as well as all other papers in these series). All the atmospheric parameters, T_{eff} , $\log g$, [Fe/H] and ξ_t , and the corresponding uncertainties, were taken from Santos et al. (2004a, 2005). The adopted solar abundances for iron, oxygen and nickel were $\log \epsilon(\text{Fe})_{\odot} = 7.47$ dex (as used in Santos et al. 2004a, 2005), $\log \epsilon(\text{O})_{\odot} = 8.74$ dex (Nissen et al. 2002), and $\log \epsilon(\text{Ni})_{\odot} = 6.25$ dex (Anders & Grevesse 1989), respectively.

3.1. The [OI] absorption at 6300 Å

A standard LTE analysis was carried out to derive oxygen abundances from the [OI] absorption at 6300.3 Å, since it is well known that this indicator is not significantly affected by deviations from LTE (e.g. Kiselman 2001). However, this line is considerably blended by an Ni I line at 6300.399 Å (e.g. Lambert 1978; Allende Prieto, Lambert & Asplund 2001). We estimated the *EW* of the Ni I line, using the *ewfind* driver of MOOG (Sneden 1973) and Ni abundances computed by Jorge et al. (private communication, see Fig. 11). The oxygen contribution has been obtained by subtracting the Ni *EW* from the whole measured *EW* of the 6300.3 Å feature. The wavelengths, excitation energies of the lower levels and oscillator strengths of the Ni I absorption were taken from Allende Prieto, Lambert

& Asplund 2001), while the adopted atomic data from [OI] are from Lambert (1978). The $\log gf$ value of the [OI] line was slightly modified in order to obtain $\log \epsilon(\text{O})_{\odot} = 8.74$. All these values are listed in Table 1. Equivalent widths were determined by Gaussian fitting using the *splot* task of IRAF, and abundances were computed with the *abfind* driver of MOOG (Sneden 1973).

Uncertainties in the atmospheric parameters are of the order of 50 K in T_{eff} , 0.12 dex in $\log g$, 0.08 km s⁻¹ in the microturbulence and 0.05 dex in the metallicity (see Santos et al. 2004a, 2005). The sensitivity of the [OI] line to variations in atmospheric parameters has been estimated as follows. We selected a set of three stars having different temperatures (HD 22049, HD 37124 and HD 9826), and we then tested abundance sensitivity to changes in each atmospheric parameter (± 100 K for T_{eff} , ± 0.3 dex for $\log g$ and [Fe/H], ± 0.05 dex for ξ_t). The results are shown in Table 2. To take into account the uncertainties caused by the continuum determination, *EWs* for the highest and the lowest continuum level were measured, and the corresponding abundance errors were added quadratically to the abundance uncertainties derived from the sensitivity to changes in the atmospheric parameters.

3.2. The OI triplet at 7771–5 Å

LTE abundances were derived from *EW* measurements of the triplet lines. The wavelengths and excitation energies of the lower levels for the three triplet lines listed in Table 1 were taken from Kurucz & Bell (1995), while oscillator strength values consistent with $\log \epsilon(\text{O})_{\odot} = 8.74$ were obtained following an inverted solar analysis in LTE. Equivalent widths were determined by Gaussian fitting using the *splot* task of IRAF, and abundances were computed with the *abfind* driver of MOOG (Sneden 1973).

NLTE corrections were calculated and applied to the LTE results. The NTE computations for the oxygen atom were carried out using the atomic model with 23 levels of O I and one level of O II. Our atomic model is based on the data of Carlsson & Judge (1993). In our computations only 31 bound–bound and 23 bound–free radiative transitions were considered; nevertheless, the consideration of additional levels and transitions does not affect our results (Shchukina 1987; Takeda 2003). It is well known that inelastic collisions with hydrogen atoms tend to offset the NLTE effects. However, it is often stated that Drawin's formalism (Drawin 1968) gives very uncertain results for hydrogen collision rates (e.g. Belyaev et al. 1999). Thus, collisions with H atoms were not taken into account in our computations. Figure 1 shows the dependence of the NLTE corrections on T_{eff} , $\log g$ and [Fe/H]. Our results are similar to those reported recently by Takeda (2003).

The sensitivity of the oxygen abundances derived from triplet lines to variations in atmospheric parameters has been estimated in the same way as in the [OI] case (see Sect. 3.1). The results are shown in Table 2. Uncertainties in the final oxygen abundances were determined adding in quadrature the abundance uncertainty resulting from the continuum determination (0.05 dex), the standard deviation of each mean

² The source code of MOOG2002 can be downloaded from <http://verdi.as.utexas.edu/moog.html>.

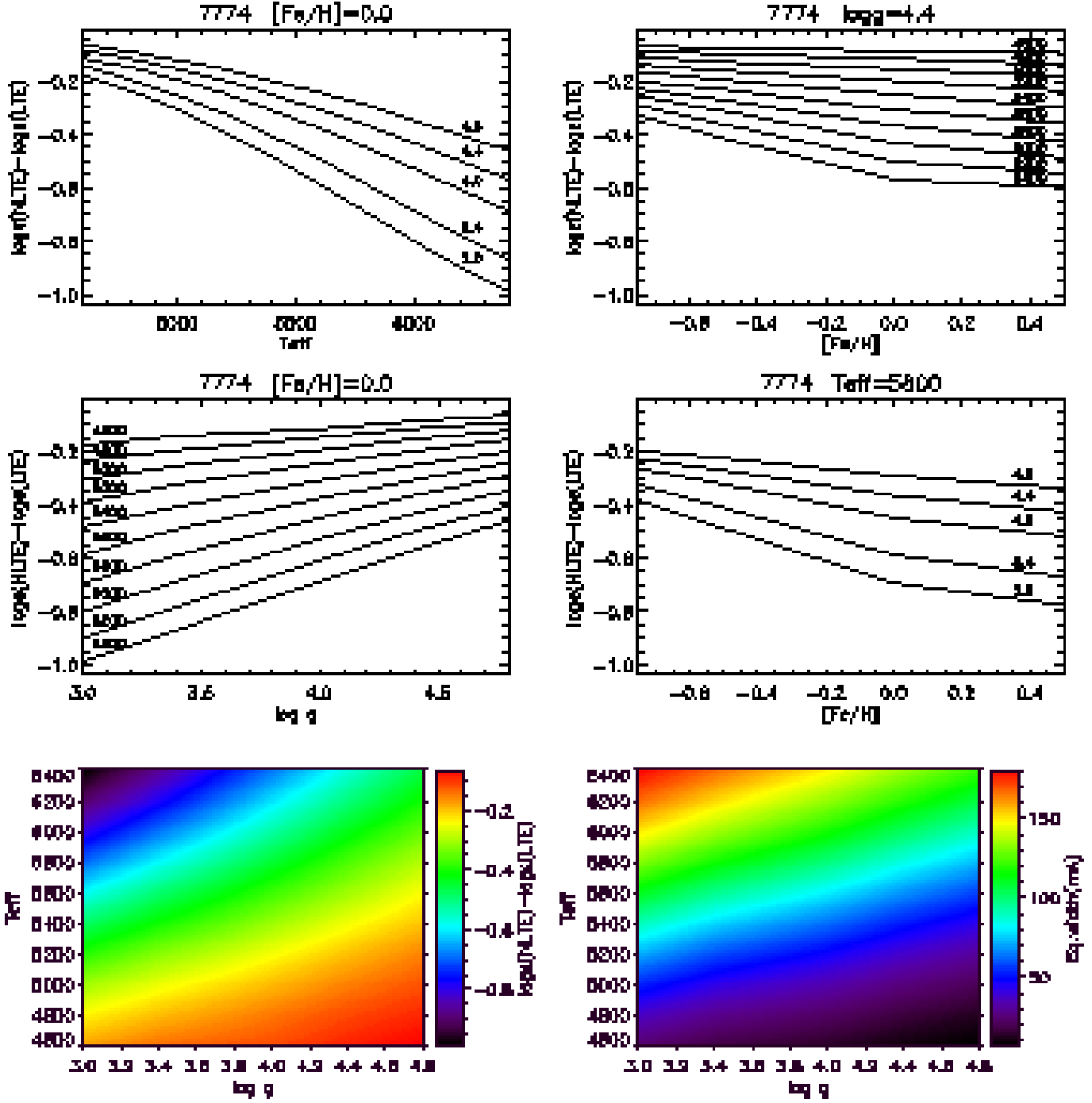


Fig. 1. NLTE abundance corrections $\log \epsilon(\text{NLTE}) - \log \epsilon(\text{LTE})$ and NLTE equivalent width of the O I IR triplet $\lambda\lambda 7774$ Å line in a grid of one-dimensional model atmospheres of Kurucz spanning the range $4600 \text{ K} < T_{\text{eff}} < 6400 \text{ K}$, $3.0 < \log g < 4.8$, and $-0.75 < [\text{Fe}/\text{H}] < 0.5$. The *right-hand top* and the *right-hand middle* panels show the results for stars with the solar-like gravity $\log g = 4.4$ and the solar-like effective temperature $T_{\text{eff}} = 5800 \text{ K}$, while the *right-hand bottom* and all the *left-hand* panels show the results for stars with the solar metallicity $[\text{Fe}/\text{H}] = 0.0$. The *bottom* panels show variations of the NLTE abundance corrections (*left*) and the NLTE equivalent width with T_{eff} and $\log g$ for $[\text{Fe}/\text{H}] = 0.0$. The numbers above curves indicate the gravities and effective temperatures.

abundance and the errors due to the abundance sensitivities to changes in the atmospheric parameters.

3.3. Synthesis of the near-UV OH lines

We determined oxygen abundances by fitting synthetic spectra to the data. Four OH features were analysed at 3167.2 Å, at 3189.3 Å, at 3255.5 Å, and at 3173 Å, composed of two

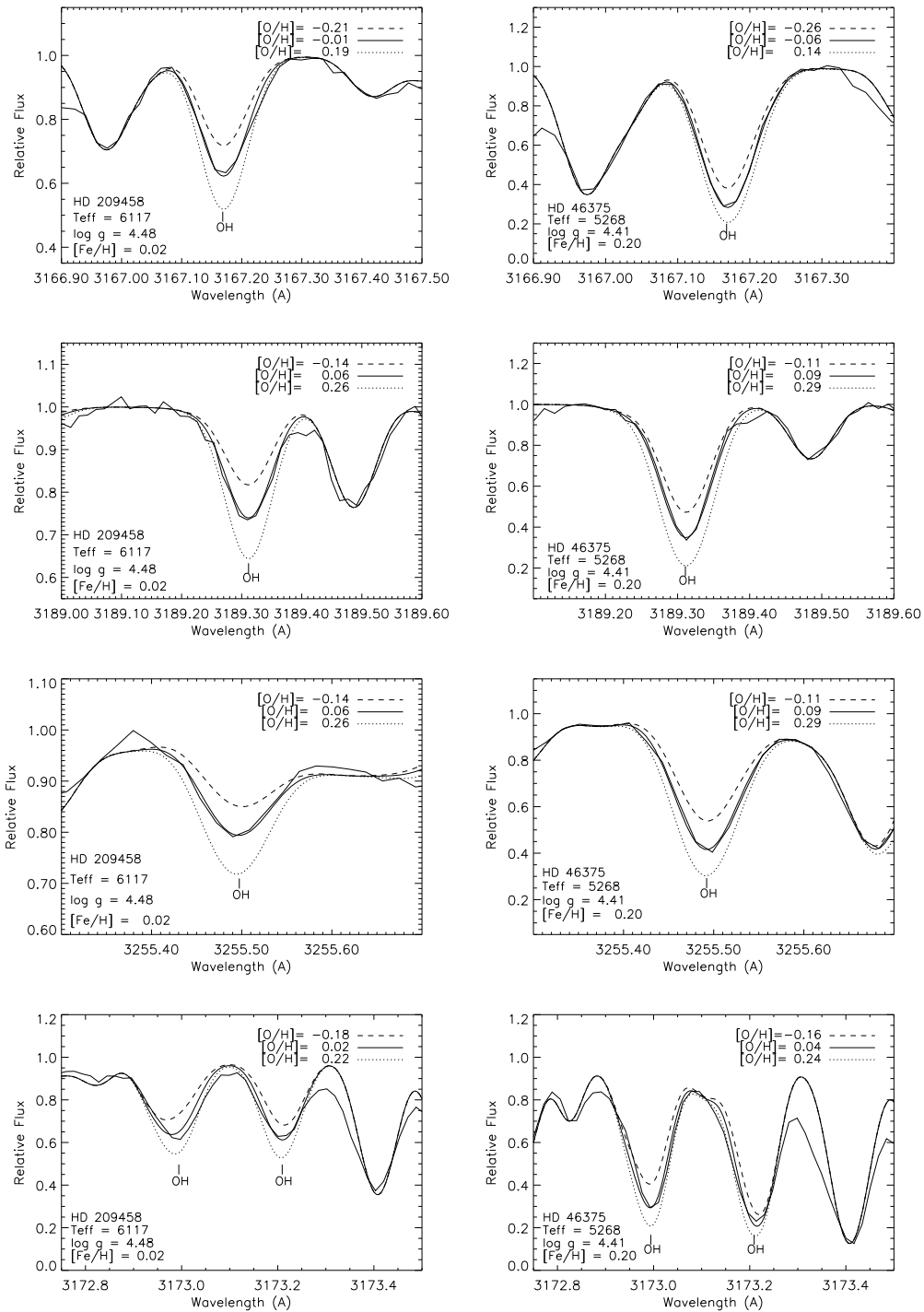


Fig. 2. The observed spectrum (thick solid line) and three synthetic spectra (dotted, dashed and solid lines) for different values of [O/Fe] in the four OH features analysed, for two targets.

OH lines, at 3172.9 Å and at 3173.2 Å. The atomic line lists for each spectral region were taken from VALD (Kupka et al. 1999), while the molecular data of the OH lines were extracted from Kurucz database.³ We assumed the dissociation potential of the OH molecule $D_0(\text{OH}) = 4.39 \text{ eV}$ (Huber & Herzberg

³ Molecular line data can be downloaded at <http://kurucz.harvard.edu/LINELISTS/LINESMOL>.

1979). Oscillator strength values were slightly modified in order to achieve a good fit to the Kurucz Solar Atlas (Kurucz et al. 1984), with a solar model having $T_{\text{eff}} = 5777 \text{ K}$, $\log g = 4.44 \text{ dex}$, and $\xi_t = 1.0 \text{ km s}^{-1}$. The adopted data are listed in Table 1.

The continuum was normalized with 5th order polynomials using the CONT task of IRAF. We then made further improvements in the placement of the continuum using the DIPSO task of the STARLINK software: some points of reference of

Table 2. Sensitivity of the three indicators [O I], O I and OH to changes of 100 K in effective temperature, 0.3 dex in gravity and metallicity, and 0.5 km s⁻¹ in microturbulence

		$\Delta T_{\text{eff}} = \pm 100 \text{ K}$	$\Delta \log g = \pm 0.3 \text{ dex}$	$\Delta [\text{Fe}/\text{H}] = \pm 0.3 \text{ dex}$	$\Delta \xi_t = \pm 0.5 \text{ km s}^{-1}$
[O I]	Star	$\Delta[\text{O/H}]$	$\Delta[\text{O/H}]$	$\Delta[\text{O/H}]$	$\Delta[\text{O/H}]$
	HD 22049	± 0.01	± 0.14	± 0.09	$\pm 0.00^1$
	HD 37124	± 0.01	± 0.14	± 0.08	$\pm 0.00^1$
	HD 9826	± 0.01	± 0.14	± 0.09	± 0.01
O I	Star	$\Delta[\text{O/H}]$	$\Delta[\text{O/H}]$	$\Delta[\text{O/H}]$	$\Delta[\text{O/H}]$
	HD 22049	∓ 0.14	± 0.09	± 0.02	∓ 0.02
	HD 37124	∓ 0.10	± 0.05	± 0.02	∓ 0.02
	HD 9826	∓ 0.07	± 0.05	± 0.02	∓ 0.03
OH	Star	$\Delta[\text{O/H}]$	$\Delta[\text{O/H}]$	$\Delta[\text{O/H}]$	$\Delta[\text{O/H}]$
	HD 22049	± 0.05	∓ 0.03	± 0.18	$\pm 0.00^1$
	HD 37124	± 0.10	∓ 0.05	± 0.20	$\pm 0.00^1$
	HD 9826	± 0.12	∓ 0.05	± 0.20	$\pm 0.00^1$

¹ These sensitivities are based on the method described in Section 3.1. The values can be slightly larger if more explicit calculations are carried out.

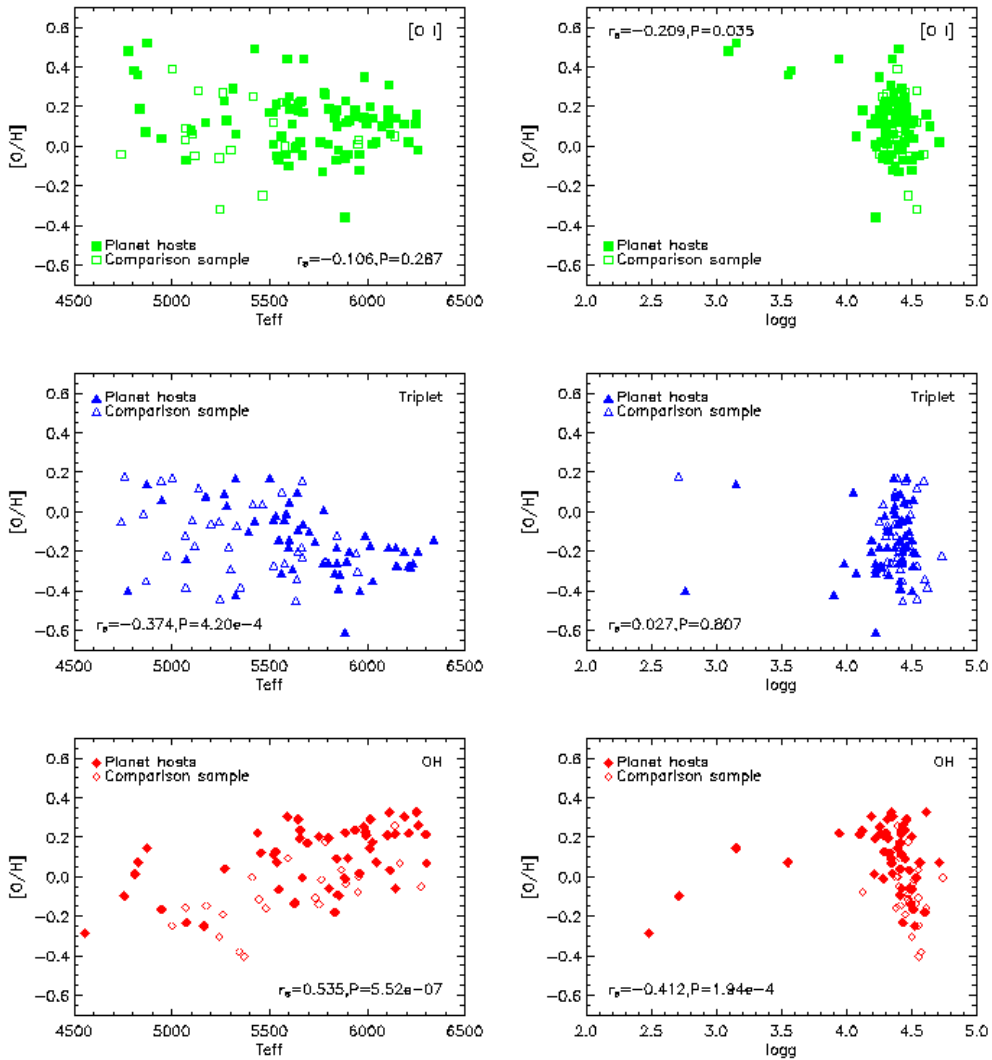


Fig. 3. [O/Fe] vs. T_{eff} and $\log g$ for the different indicators. Filled and open symbols represent planet host and comparison sample stars, respectively. The Spearman rank-order correlation coefficient and its significance value are written at the bottom of each plot.

the continuum level were selected in the Kurucz Solar Flux Atlas (Kurucz et al. 1984) and used in the determination of the stellar continuum of our observed spectra. For the instrumental broadening we used a Gaussian function with $FWHM$ of 0.05 Å and a rotational broadening function with $v \sin i$ values from CORALIE database. All our targets are slow rotators, with $v \sin i$ values between 1 and 5 km s $^{-1}$ in almost all cases. No macroturbulence broadening was used. Two examples of the fitting of the four features are shown in Figure 2.

The sensitivity of the oxygen abundances from OH lines to changes in the atmospheric parameters was estimated in the same way as for the [OI] and OI indicators (see Sect. 3.1 and Sect. 3.2). Uncertainties derived from inaccuracies in atmospheric parameters were added in quadrature to the abundance uncertainty resulting from the continuum determination (0.05 dex) and to the standard deviation of each mean abundance.

The dependence on T_{eff} and on $\log g$ of the [O/H] results from all the indicators is represented in Figure 3. We note that no significant trends appear for [OI] and OH. This means that our results are almost free from systematic errors. Only in the case of triplet, does a trend of decreasing [O/H] with increasing T_{eff} exist. This is probably due to the high dependence on T_{eff} of the NLTE corrections applied to the LTE results of the triplet.

4. Comparison between different indicators

Abundances from the [OI] line at 6300 Å were obtained in 103 dwarfs (see Tables 4 and 5), while 77 stars were analysed using near-UV OH lines (see Table 6 and 7). LTE abundances were derived from the triplet lines at 7771–5 Å and then corrected for NLTE effects for 87 stars (see Tables 8 and 9). Altogether we present oxygen abundances derived from these three indicators for 96 and 59 stars with and without known planets, respectively.

4.1. Triplet vs. [OI] and near-UV OH

Figure 4 (top panel) shows the comparison between the results obtained from the NLTE study of the 7771–5 Å triplet and the analysis of the [OI] 6300 Å line. NLTE triplet abundances are systematically lower with respect to the forbidden-line results, with discrepancies of the order of 0.3 dex on average.

The values obtained from the synthesis of OH lines present a better consistency with the NLTE triplet results (see Figure 4, middle panel). In this case, the comparison is less meaningful because of the limited number of targets in common between the two analyses. Nevertheless, a large portion of targets show underabundances of the order of 0.2 dex in NLTE triplet values with respect to near-UV OH results.

The NLTE corrections applied to the LTE analysis results correspond to the maximum effect, since collisions with H atoms are not taken into account (see Sect. 3.2). This can produce an underestimation of the final triplet abundances, and could be the reason for the systematic underabundance of the NLTE triplet results.

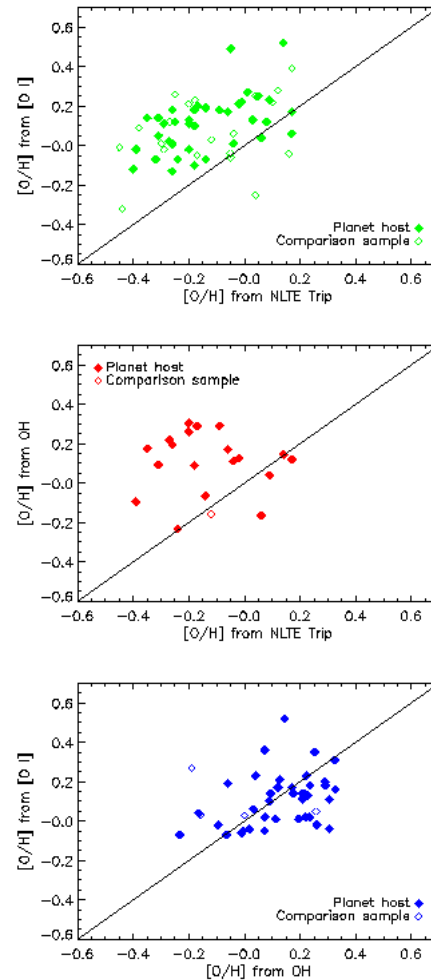


Fig. 4. Comparisons of the results from different indicators: [OI] line, OH lines and triplet lines in NLTE.

If we compare results from LTE triplet analysis with those from [OI] 6300 Å and OH (see Figure 5), the consistency with these indicators improves, with typical discrepancies of 0.1 dex. Moreover, a suggestive number of targets shows an overabundance of the order of 0.2 dex in LTE triplet values. This means that the NLTE and LTE analyses give lower and upper limits, respectively, for the oxygen abundance.

4.2. [OI] vs. near-UV OH

Figure 4 (bottom panel) represents the comparison between oxygen abundances obtained from the analysis of the [OI] 6300 Å line and from the synthesis of near-UV OH lines. In most cases the two indicators agree quite well, with discrepancies of the order of 0.1 dex. Abundances obtained from OH lines are generally lower than those from the 6300 Å [OI] line.

The cause of this behaviour could be an underestimation of the Ni I component blended with the 6300 Å [OI] line. The atomic parameters, especially the $\log gf$, for this Ni I line are uncertain (e.g. Allende Prieto, Lambert & Asplund 2001), and this can introduce uncertainties in the estimation of the Ni I line contribution to the total spectral feature at 6300.3 Å.

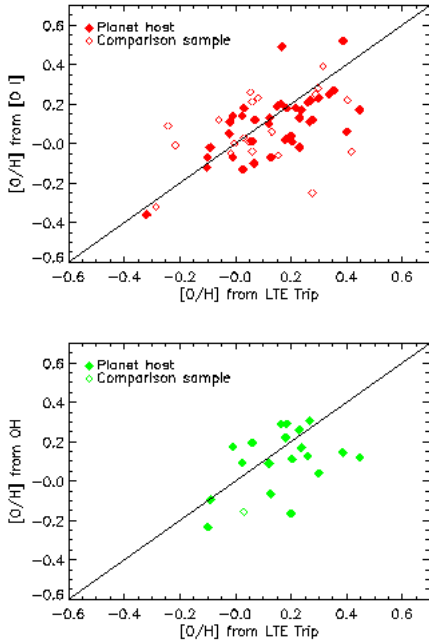


Fig. 5. Comparisons of the results from [OI] and OH lines with those obtained from triplet lines in LTE.

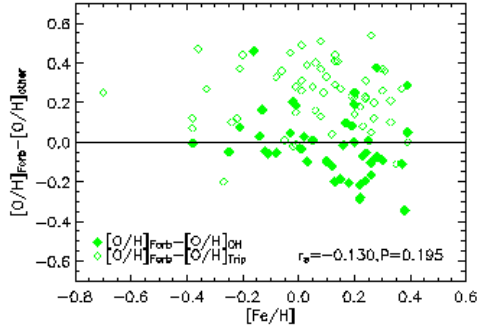


Fig. 6. Difference between [O/H] ratios derived from [OI] and from another indicator, OH (filled symbols) or triplet (open symbols), vs. [Fe/H]. The Spearman rank-order correlation coefficient and its significance value are written at the bottom of the plot.

Moreover, dwarfs have very weak [OI] lines (e.g. $EW \sim 5$ mÅ in the Sun). Thus, measurement uncertainties may be very large, depending on the resolution and S/N of the data.

If the uncertainties related to Ni I were the main responsible of the discrepancies with the other two indicators, a correlation should exist between these discrepancies and metallicity. Figure 6 shows the difference of abundances from [OI] and from other indicators as a function of [Fe/H], as well as the correlation coefficient and its significance value. Since no correlation with metallicity exists, we can discard the possibility that the Ni I blend introduces significant errors into our [OI] results.

Another source of uncertainty could be the strong dependence of the OH lines on temperature, and therefore to surface

Table 3. Average [O/H] values from the different indicators, with the corresponding dispersions, for the set of planet host stars and the comparison sample

Indicator	$\langle [O/H] \rangle \pm rms$ (comp. sample)	$\langle [O/H] \rangle \pm rms$ (planet hosts)	Difference
OH	-0.07 ± 0.16	0.10 ± 0.16	0.17
[OI]	0.07 ± 0.17	0.12 ± 0.16	0.05
NLTE OI	-0.14 ± 0.18	-0.16 ± 0.17	-0.02
LTE OI	0.08 ± 0.20	0.15 ± 0.17	0.07
mean(NLTE)	-0.07 ± 0.16	0.03 ± 0.18	0.10
mean(LTE)	-0.07 ± 0.16	0.12 ± 0.16	0.19

inhomogeneities. However, previous works (e.g. Israeli et al. 1998; Boesgaard et al. 1999; Ecuvillon et al. 2004a) obtained a good consistence between abundances based on molecular and atomic features using classical 1D atmosphere models. This fact, added to the agreement we have found between [OI] and OH measures, makes us confident about the reliability of our OH results. We found that discrepancies between OH, OI triplet and [OI] barely exceed 0.2 dex.

5. Comparison between planet host and comparison sample stars

Several studies have been published about abundances of metals other than iron in planet host stars (Santos et al. 2000; Gonzalez et al. 2001; Takeda et al. 2001; Sadakane et al. 2002; Bodaghee et al. 2003; Ecuvillon et al. 2004a, 2004b). Oxygen abundances have been analysed by some of them (Santos et al. 2000; Gonzalez et al. 2001; Takeda et al. 2001; Sadakane et al. 2002; Takeda & Honda 2005). However the limited number of planet host stars considered, and the comparison realized by some authors between targets with planets and field stars extracted from the literature, have prevented definitive conclusions from being reached.

We have carried out a homogeneous study of oxygen abundances in an almost complete set of 96 stars with extrasolar giant planets, as well as in a large volume-limited sample of 59 stars with no known planetary-mass companion, all belonging to the CORALIE planet search survey (see Udry et al. 2000). The volume-limited comparison sample consists of stars from the CORALIE southern planet search sample without any known planets, with distances below 20 pc, as derived from *Hipparcos* parallaxes (ESA 1997). All these stars and their parameters come from Santos et al. (2001, 2003b, 2004a, 2005). Three different indicators were used in order to obtain more reliable and solid results.

5.1. [O/H] distributions

Figure 7 presents [O/H] distributions of the two samples, stars with and without planets, for the different indicators: [OI] 6300 Å (left top panel), near-UV OH (top right panel) and triplet 7771–5 Å with NLTE (bottom left panel) and LTE (bottom right panel) treatments. Forbidden line results for the compar-

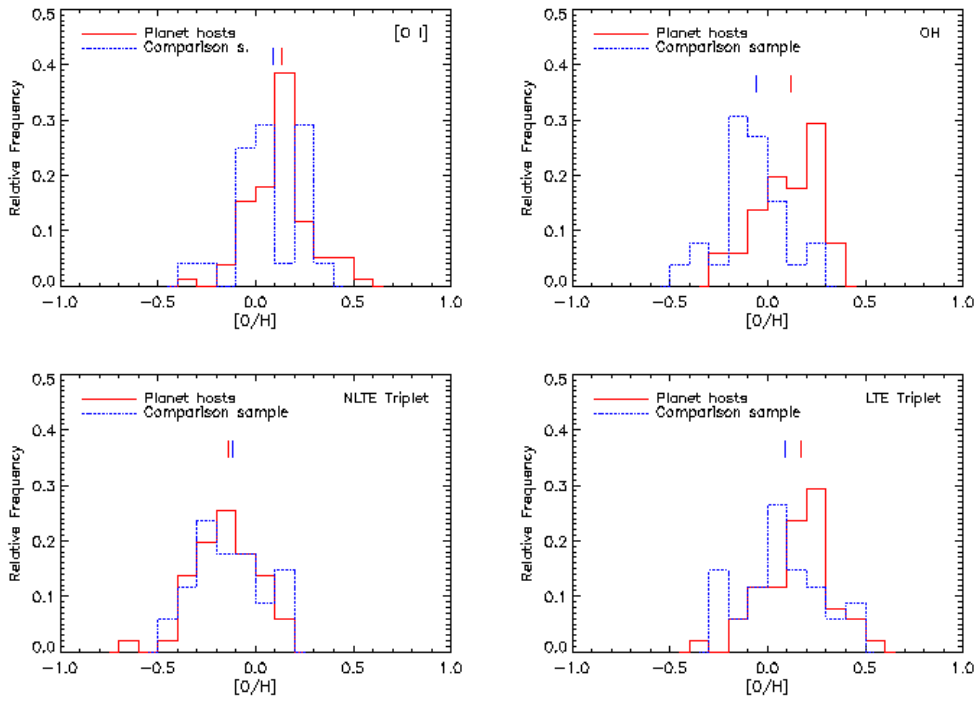


Fig. 7. [O/H] distributions from different indicators. The solid and dotted lines represent planet host and comparison sample stars, respectively. The vertical lines represent the average abundance values of the two samples, stars with and without planets.

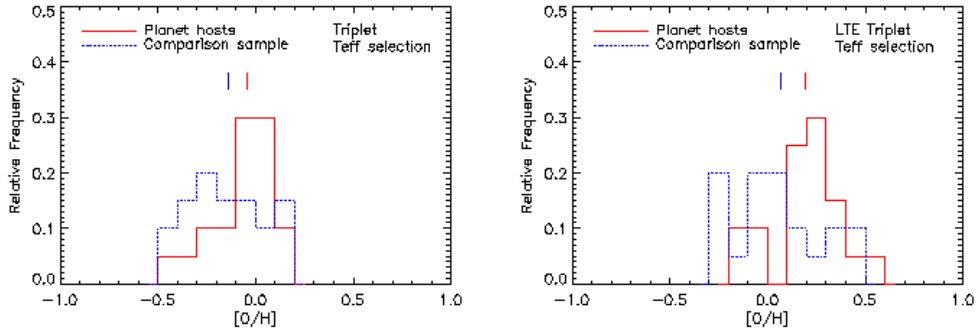


Fig. 8. [O/H] distributions for NLTE (left panel) and LTE (right panel) triplet results for the two subsamples of planet host (solid line) and comparison sample (dotted line) stars with the *same* T_{eff} distributions. The vertical lines represent the average abundance values of the two subsamples, stars with and without planets.

ison sample present a bimodal shape, characterized by a steep descent from the peak around $[O/H] \sim 0.0$ towards negative values. The distribution of planet host stars obtained with the same indicator exhibits a symmetrical shape, with a steep descent from the peak around $[O/H] \sim 0.2$ towards $[O/H] > 0.2$. An asymmetric distribution is obtained from the OH results for planet host stars, while the comparison sample has a symmetric shape (see Figure 7, top right panel). The NLTE and LTE triplet distributions are quite symmetrical for the two samples of stars with and without planets (see Figure 7, bottom panels).

The average values of [O/H] for the samples with and without planets for each indicator, and for all the indicators together, as well as the rms dispersions and the differences between the mean [O/H] values, are listed in Table 3. In general, the mean [O/H] value corresponding to the comparison sample is lower

than the mean abundance value obtained for the set of planet host stars. From the [OI] analysis we obtain a difference of the order of 0.05 dex between the mean abundances of the two samples, while the OH synthesis leads to a larger difference of 0.17 dex.

The NLTE triplet values present a particular characteristic: the mean abundance value is lower in planet host stars than in the comparison sample. This could be because the comparison stars with available triplet measurements are generally cooler than planet host stars with triplet determinations, and NLTE corrections are much less important for lower T_{eff} . The abundance underestimation related to our NLTE treatment (see Sect. 4.1) is therefore on average less significant in the comparison sample than in the planet host stars. In fact, if we select two subsamples of stars with and without planets hav-

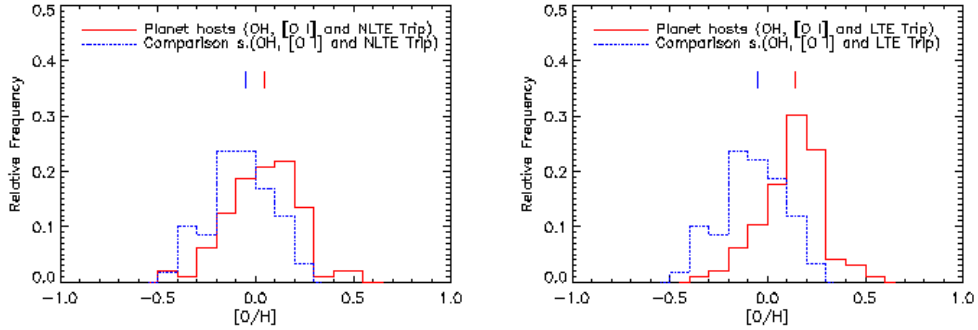


Fig. 9. Left panel: [O/H] distributions using average results from OH lines, [O I] line and O I triplet in NLTE. Right panel: [O/H] distributions using average results from OH lines, [O I] line and O I triplet in LTE. The solid and dotted lines represent planet host and comparison sample stars, respectively. The vertical lines represent the average abundance values of the two samples, stars with and without planets.

ing the same T_{eff} distributions, and compare their triplet [O/H] distributions, this effect disappears (see Figure 8). The planet host subsample shows an average oxygen overabundance of the order of 0.1 dex with respect to the comparison subsample, in both NLTE (Figure 8, left panel) and LTE (Figure 8, right panel) analyses.

Figure 9 presents the [O/H] distributions of the two samples, stars with and without planets, obtained by averaging for each target the abundances obtained from different indicators, adopting NLTE (left panel) or LTE (right panel) triplet values. The distributions of the comparison sample obtained in both cases are very similar: both have slightly asymmetric shapes, with mean values of -0.10 dex. Concerning the planet host sample, both distributions issued from including NLTE and LTE triplet values, respectively, show asymmetric shapes. The latter present a mean value ($\langle [O/H] \rangle = 0.12$) much larger than the former ($\langle [O/H] \rangle = 0.03$ – see Table 3). As our NLTE treatment considers maximum NLTE corrections, we may consider the abundances obtained from including the NLTE and LTE triplet values to correspond to lower and upper limits, respectively (see Sect. 4.1). Therefore we propose that planet host stars present an average oxygen overabundance between 0.1 and 0.2 dex with respect to the comparison sample.

5.2. [O/H] and [O/Fe] vs. [Fe/H]

In Figure 10, [O/Fe] and [O/H] ratios as functions of [Fe/H] for [O I] 6300 Å (top panel), O I 7771–5 Å (middle panel), and near-UV OH (bottom panel) are presented. No clear differences appear between the behaviours of the two samples, stars with and without planets. There seem to be no anomalies in oxygen abundances related to the presence of planets. The average trends that planet host stars mark are similar to those traced by the comparison sample, although discrepancies between the two trends are slightly larger for the triplet than for the other indicators. Since targets with planets are on average more metal rich than comparison sample stars, their abundance distributions correspond to the extensions of the comparison sample trends at high [Fe/H].

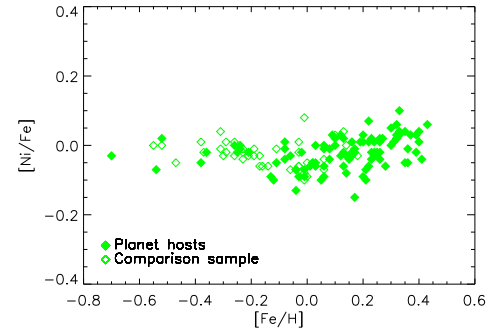


Fig. 11. [Ni/Fe] vs. [Fe/H] plot. Filled and open symbols represent planet host and comparison sample stars, respectively.

The average trends resulting from different indicators present slight discrepancies, but similar behaviours. The abundances obtained from OH line synthesis present less dispersion than those derived from the other two indicators. The [O/Fe] vs. [Fe/H] plots for all the indicators show that, on average, [O/Fe] clearly decreases with [Fe/H] in the metallicity range $-0.8 < [Fe/H] < 0.5$, with significantly negative slopes in all the linear least-squares fits. The linear least-squares fit for the [O/Fe] values averaged from the three indicators gives a slope of -0.50 ± 0.04 .

Bensby, Feltzing & Lundström (2004) obtained a similar trend of decreasing [O/Fe] with increasing [Fe/H] by analyzing [O I] in a large set of disk dwarfs. This behaviour could be caused by the steep rise these authors found in [Ni/Fe] vs. [Fe/H] for $[Fe/H] > 0$. Nevertheless, since our [Ni/Fe] vs. [Fe/H] plot does not show such a obvious increase (see Fig. 11), it is very unlikely that our [O I] results are affected by this phenomenon. Moreover, the three indicators reproduce similar steep descents, which additionally supports that the [O/Fe] decrease with increasing [Fe/H] found from [O I] analysis is “real”.

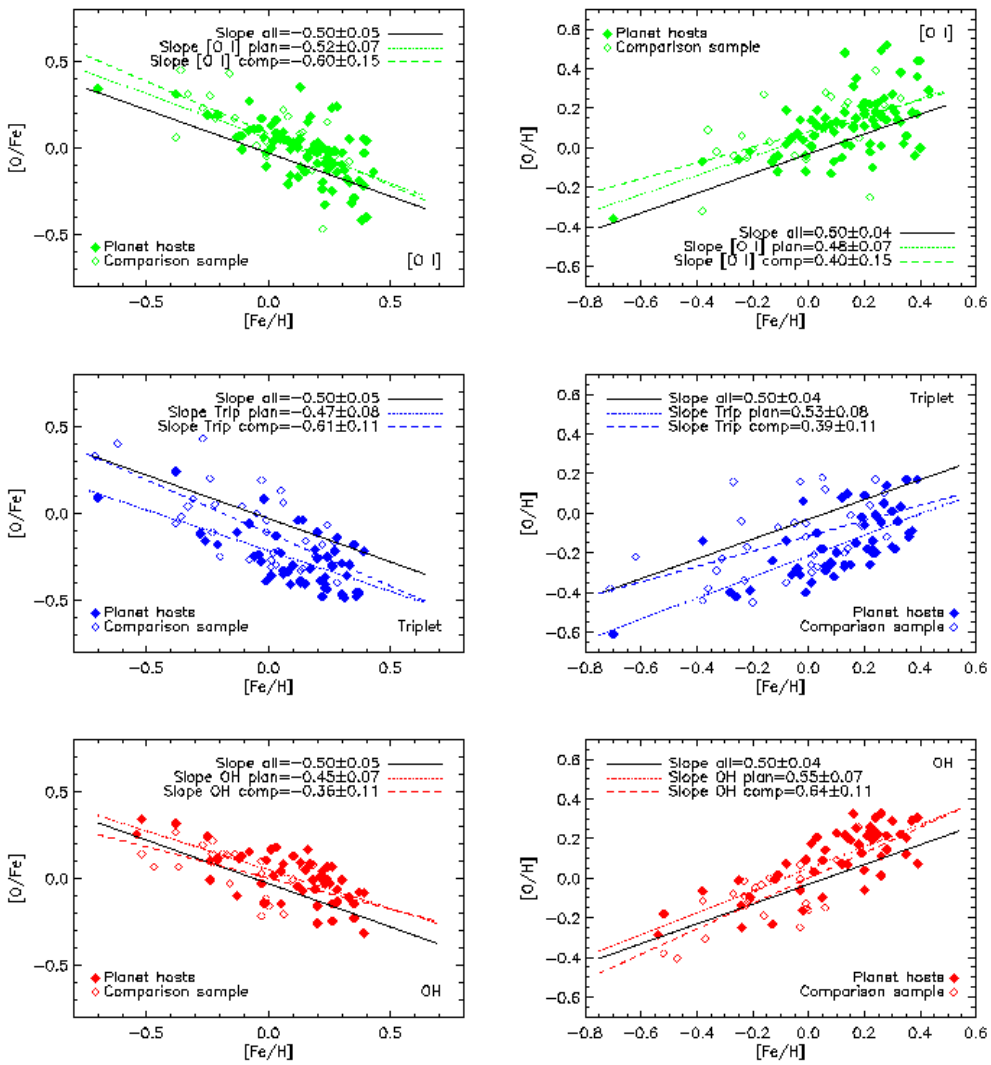


Fig. 10. [O/Fe] and [O/H] vs. [Fe/H] plots for the three indicators. Filled and open symbols represent planet host and comparison sample stars, respectively. Linear least-squares fits to both samples, stars with and without planets, for each indicator and for the three indicators together are represented and slope values are indicated at the bottom of each plot.

6. Galactic trends or effects related with planets?

The abundances of volatile elements are a key factor in searching for chemical anomalies associated with the presence of planets. If the accretion of large amounts of planetary material were the dominant source of the metallicity excess observed in planet host stars, a relative overabundance of refractory elements with respect to volatiles, or at least some anomaly related to the presence of planets, would be expected in the majority of these kinds of targets (e.g. Smith et al. 2001). Thus knowing how the abundances of volatile and refractory elements behave in stars with and without planets can give valuable clues to the relative importance of the differential accretion.

Our results show that the oxygen abundances do not present clear anomalies in planet host stars with respect to comparison sample dwarfs. The trends traced by the two samples, stars with and without planets, are nearly indistinguishable. This supports the “primordial” hypothesis suggested by Santos et al. (2000, 2001), which proposes the high metal content of the proto-

planetary cloud the system planets-star has formed out of as an explanation for the observed iron overabundance in planet-harbouring stars. Likewise, although the occurrence of accretion is not excluded, the possibility that pollution is the principal source of the observed metallicity enhancement is unlikely. Therefore the observed trends would simply be a product of the chemical evolution of the Galaxy.

Previous studies have already led to results supporting a “primordial” origin of the iron excess in planet host stars (Pinsonneault, DePoy & Coffee 2001; Santos et al. 2001, 2003b, 2004a, 2005). Takeda et al. (2001) and Sadakane et al. (2002) found no differences between the abundances of some refractory and volatile elements for a set of planet host stars and some field dwarfs from the literature. Recently, Ecuvillon et al. (2004a, 2004b) have found that the volatiles N, C, S, and Zn behave identically in a large set of planet host and comparison sample stars analysed homogeneously. Similar results have

been found by Takeda & Honda (2005) for CNO abundances in a set of 27 planet host stars.

We have also obtained a clear monotonic decrease of [O/Fe] with [Fe/H] in the metallicity range $-0.8 < [\text{Fe}/\text{H}] < 0.5$ for all the spectroscopic indicators. The corresponding linear least-squares fits have significantly negative slopes, with values around -0.5 . Some previous studies of oxygen abundances in Galactic disc stars (Nissen & Edvardsson 1992; Edvardsson et al. 1993; Nissen et al. 2002) found [O/Fe] ratios flattening in the metallicity range $-0.3 < [\text{Fe}/\text{H}] < 0.3$. Nevertheless, further studies have revealed that oxygen continues to decline with increasing [Fe/H] (e.g. Feltzing & Gustafsson 1998; Takeda 2003). A recent analysis of a large number of F and G disk dwarfs by Bensby, Feltzing & Lundström (2004) has obtained a monotonic decrease of [O/Fe] ratios in the metallicity range $-0.9 < [\text{Fe}/\text{H}] < 0.4$, which is in concordance with the predictions of chemical evolution models of the Milky Way (e.g. Chiappini et al. 2003). This implies that oxygen is produced only in SNe II, with no SN Ia signature contribution, which would produce a levelling out of [O/Fe] at $[\text{Fe}/\text{H}] = 0$, as has been observed in other α -elements (Bensby, Feltzing & Lundström 2003, 2004). Takeda & Honda (2005) have found [O/Fe] increasing with decreasing [Fe/H] with a slope of $\sim 0.4 - 0.5$ for a large sample of 160 dwarfs with metallicities $-1 < [\text{Fe}/\text{H}] < +0.4$. Our study has obtained a similar monotonic decrease and thus confirms this issue.

An average oxygen overabundance of between 0.1 and 0.2 dex in the planet host stars with respect to the comparison sample has been obtained. It is not clear if this difference is due to the presence of planets. In order to check this possibility, models of Galactic chemical evolution in this metallicity range must be studied. Unfortunately, such models are not available, and our conclusions can only be based on the best guess. For example, assuming that the main parameters which govern the trends of chemical elements in the galactic disk do not vary in the metallicity range $-1 < [\text{Fe}/\text{H}] < 0.5$, we would expect that the elements of the same nucleosynthetic origin present similar behaviours at super-solar metallicities. However, this is not what is observed. For instance, the [X/Fe] ratios of the α -elements Si, Ti and Mg decrease monotonically in the metallicity range $-1 < [\text{Fe}/\text{H}] < 0$ and become constant in the super-solar regime (e.g. Bodaghee et al. 2003; Gilli et al. 2005), while, as we have seen above, the [O/Fe] ratio continuously decreasing in the whole metallicity range. Since at these metallicities the fraction of planet-harbouring stars is important, we cannot exclude the possibility of global effects on abundance trends linked to planets. More works needs to be done before we can tackle this problem.

7. Concluding remarks

We presented the first detailed and uniform study of oxygen abundances in an almost complete set of planet-harbouring stars and in a unbiased volume-limited comparison sample of solar-type dwarfs with no known planetary-mass companions. An homogeneous set of atmospheric parameters, spectroscopically determined, was adopted, and three independent analyses from different indicators were performed. We also provide the

first accurate and homogeneous comparison of near-UV OH, 6300 Å [OI] and 7771–5 Å OI triplet in a large set of solar-type stars.

Oxygen is one of the most controversial elements due to its problematic indicators. We found a good agreement between the results of [OI] and OH analyses. The NLTE treatment for the triplet led to an underestimation of the oxygen abundances, while the LTE values may be considered as abundance upper limits. The OH results show a much smaller dispersion in the [O/Fe] and [O/H] vs. [Fe/H] plots with respect to the others values, while the [OI] analysis generally reveals a better agreement with other indicators.

We found that [O/Fe] and [O/H] trends as function of metallicity show the same behaviour in planet host and comparison sample stars. No anomalies associated with the presence of planets have appeared in those representations. For all the indicators, [O/Fe] ratios decrease monotonically with [Fe/H], with significantly negative slopes of the order of -0.5 . Planet host stars present on average an oxygen overabundance between 0.1 and 0.2 dex with respect to the comparison sample.

We have discussed whether these characteristics are effects related to the presence of planets or products of Galactic chemical evolution. Further investigations on the refractory/volatile abundance ratios in stars with and without planets, as well as detailed comparisons with theoretical models at super-solar metallicities, are required to provide more conclusive evidence for the debate.

Acknowledgements. The authors acknowledge the data analysis facilities provided by the Starlink Project which is run by CCLRC on behalf of PPARC. We thank the referee Dr. P. E. Nissen for many useful suggestions and comments. Support from Fundação para a Ciência e a Tecnologia (Portugal) to N.C.S. in the form of a scholarship (reference SFRH/BPD/8116/2002) and a grant (reference POCI/CTE-AST/56453/2004) is gratefully acknowledged.

References

- Abia, C., & Rebolo, R. 1989, ApJ, 347, 186
- Allende Pireto, C., Lambert, D. L., & Asplund, M. 2001, ApJ, 556, 63
- Anders, E., & Grevesse, N. 1989, Geochim. Acta, 53, 197
- Arnett, W. D. 1978, ApJ, 219, 1008
- Asplund, M., Grevesse, N., Sauval, A. J., Allende Prieto, C., & Kiselman, D. 2004, A&A, 417, 751
- Beirao, P., Santos, N. C., Israeli, G., & Mayor, M. 2005, A&A, in press, astro-ph/0504157
- Belyaev, A. K., Grosser, J., Hahne, J., & Menzel, T. 1999, Phys. Rev., 60, 2150
- Bensby, T., Feltzing, S., & Lundström, I. 2003, A&A, 410, 527
- Bensby, T., Feltzing, S., & Lundström, I. 2004, A&A, 415, 155
- Bessell, M.S., Sutherland, R. S., & Ruan, K. 1991, ApJ, 383, L71
- Bodaghee, A., Santos, N. C., Israeli, G., & Mayor, M. 2003, A&A, 404, 715
- Boesgaard, A. M., King, J. R., Deliyannis, C. P., & Vogt, S. S. 1999, AJ, 117, 492
- Cavallo, R. M., Pilachowski, C. A., & Rebolo, R. 1997, PASP, 109, 226
- Carlsson, M., & Judge, P. 1993, ApJ, 402, 344
- Chiappini, C., Romano, D., & Matteucci, F. 2003, MNRAS, 339, 63
- Drawin, H.-W. 1968, Z. Phys., 211, 404

- Ecuvillon, A., Israeli, G., Santos, N.C., Mayor, M., R. J. García López, Randich, S., 2004a, *A&A*, 418, 703
- Ecuvillon, A., Israeli, G., Santos, N.C., Mayor, M., Villar, V., & Biham, G. 2004b, *A&A*, 426, 619E
- Edvardsson, B., Andersen, J., Gustafsson, B., Lambert, D. L., Nissen, P. E., & Tomkin, J. 1993, *A&A*, 275, 101
- Feltzing, S., & Gustafsson, B. 1998, *A&AS*, 129, 237
- Fulbright, J. P., & Johnson, J. A. 2003, *ApJ*, 595, 1154
- Gilli, G., Israeli, G., Ecuvillon, A., Santos, N.C., & Mayor, M. 2005, *A&A*, in preparation
- Gonzalez, G. 1997, *MNRAS*, 285, 403
- Gonzalez, G., & Laws, C. 2000, *AJ*, 119, 390
- Gonzalez, G., Laws, C., Tyagi, S., & Reddy, B. E. 2001, *AJ*, 121, 432
- Huber, K. P., & Herzberg, G. 1979, Constants of Diatomic Molecules (New York: Van Nostrand Reinhold)
- Israeli, G., Rebolo, R., García-López, R. J., Bonifacio, P., Molero, P., & Shchukina, N. 2001a, *ApJ*, 551, 833
- Israeli, G., Santos, N. C., Mayor, M., & Rebolo, R. 2001b, *Nature*, 411, 163
- Israeli, G., García-López, R. J., & Rebolo, R. 1998 *ApJ*, 507, 805
- Israeli, G., Santos, N. C., Mayor, M., & Rebolo, R. 2003a, *A&A*, 405, 753
- Israeli, G. 2003b, in IAU S219: Stars as Suns: Activity, Evolution, and Planets, ed. A. K. Dupree (San Francisco: ASP), in press
- Israeli, G., Santos, N. C., Mayor, M., & Rebolo, R. 2004a, *A&A*, 414, 601
- Israeli, G., Shchukina, N., Rebolo, R., Basri, G., González Hernández, J. I., & Kajino, T. 2004b, *A&A*, 419, 1095
- King, J. R., & Boesgaard, A. M. 1995, *AJ*, 109, 383
- Kiselman, D. 1991, *A&A*, 245, L9
- Kiselman, D. 1993, *A&A*, 275, 269
- Kiselman, D., & Nordlund, Å. 1995, *A&A*, 302, 578
- Kiselman, D. 2001, *New Ast. Rev.*, 45, 559
- Kupka, F. G., Piskunov, N. E., Ryabchikova, T. A., Stempels, H. C., & Weiss, W. W. 1999, *A&AS*, 138, 119
- Kurucz, R. L. 1993, CD-ROMs, ATLAS9 Stellar Atmospheres Programs and 2 km s⁻¹ Grid (Cambridge: Smithsonian Astrophys. Obs.)
- Kurucz, R. L., & Bell, B. 1995, Kurucz CD-ROM No.23 (Harvard-Smithsonian Center for Astrophysics)
- Kurucz, R. L., Furenlid, I., Brault, J., Testerman, L. 1984, Solar Flux Atlas from 296 to 1300 nm, NOAO Atlas No. 1
- Lambert, D. L. 1978, *MNRAS*, 182, 249
- Laws, C., Gonzalez, G., Walker, K. M., Tyagi, S., Dodsworth, J., Snider, K. & Suntzeff, N. 2003, *AJ*, 125, 2664
- McWilliam, A. 1997, *ARA&A*, 35, 503
- Mishenina, T., Korotin, S., Klochkova, V., & Panchuk, V. 2000, *A&A*, 353, 978
- Nissen, P. E., & Edvardsson, B. 1992, *A&A*, 261, 255
- Nissen, P.E., Gustafsson, B., Edvardsson, B., & Gilmore, G. 1994, *A&A*, 285, 440
- Nissen, P. E., Primas, F., Asplund, M., & Lambert, D. L. 2002, *A&A*, 390, 235
- Pinsonneault, M. H., DePoy, D. L., & Coffee, M. 2001, *ApJ*, 556, 59
- Prochaska, J. X., Naumov, S. O., Carney, B. W., McWilliam, A., & Wolfe, A. M. 2000, *ApJ*, 120, 2513
- Sadakane, K., Ohkubo, Y., Takeda, Y., Sato, B., Kambe, E., & Aoki, W. 2002, *PASJ*, 54, 911
- Sandquist, E. L., Dokter, J. J., Lin, D. N. C., & Mardling, R. 2002, *ApJ*, 572, 1012
- Santos, N. C., Israeli, G., & Mayor, M. 2000, *A&A* 363, 228
- Santos, N. C., Israeli, G., & Mayor, M. 2001, *A&A* 373, 1019
- Santos, N. C., García López, R. J., Israeli, G., Mayor, M., Rebolo, R., García-Gil, A., Pérez de Taoro, M. R., & Randich, S. 2002, *A&A*, 386, 1028
- Santos, N. C., Mayor, M., Udry, S., et al., 2003a, in IAU S219: Stars as Suns: Activity, Evolution, and Planets, ed. A. K. Dupree (San Francisco: ASP), in press
- Santos, N. C., Israeli, G., Mayor, M., Rebolo, R., & Udry, S. 2003b, *A&A*, 398, 363
- Santos, N. C., Israeli, G., & Mayor, M. 2004a, *A&A*, 415, 1153
- Santos, N.C., Israeli, G., García López, R. J., Mayor, M., Rebolo, R., Randich, S., Ecuvillon, A., & Domínguez Cerdeña, C. 2004b, *A&A*, 427, 1085
- Santos, N. C., Israeli, G., Mayor, M., Bento, J. P., Almeida, P.C., Sousa, S. G., & Ecuvillon, A. 2005, *A&A*, in press
- Shchukina, N. 1987, *Kinemat. Phys. Cel. Bod.*, 3(6), 36
- Shchukina, N. G., Trujillo Bueno, J., & Asplund, M. 2005, *ApJ*, 618, 939
- Smith, V. V., Cunha, K., & Lazzaro, D., 2001, *AJ*, 121, 3207
- Sneden, C. 1973, Ph.D. thesis, University of Texas
- Takeda, Y., Sato, B., Kambe, E., Aoki, W., Honda, S., Kawanomoto, S., & Masuda, S., et al. 2001, *PASJ*, 53, 1211
- Takeda, Y. 2003, *A&A*, 402, 343
- Takeda, Y. & Honda, S. 2005, *PASJ*, 57, 65
- Tinsley, B. M. 1979, *ApJ*, 229, 1046
- Tomkin, J., Lemke, M., Lambert, D. L., & Sneden, C. 1992, *AJ*, 104, 1568
- Udry, S., Mayor, M., Naef, D., et al. 2000, *A&A*, 356, 590
- Woosley, S. E., & Weaver, T. A. 1995, *ApJS*, 101, 181

Table 4: Oxygen abundances from [OI] line in a set of planet host stars.

Star	T_{eff} (K)	$\log g$ (cm s^{-2})	ξ_t (km s^{-1})	[Fe/H]	$\text{EW}_{[\text{OI}]}$ (mÅ)	$[\text{O}/\text{H}]_{[\text{OI}]}$	Instr.
HD 1237	5536 ± 50	4.56 ± 0.12	1.33 ± 0.06	0.12 ± 0.06	2.9 ± 0.5	-0.05 ± 0.10	[1]
HD 23079	5959 ± 46	4.35 ± 0.12	1.20 ± 0.10	-0.11 ± 0.06	3.5 ± 0.5	-0.12 ± 0.09	[1]
HD 28185	5656 ± 44	4.45 ± 0.08	1.01 ± 0.06	0.22 ± 0.05	5.4 ± 0.8	0.22 ± 0.09	[1]
HD 30177	5591 ± 50	4.35 ± 0.12	1.03 ± 0.06	0.39 ± 0.06	8.3 ± 0.5	0.44 ± 0.07	[1]
HD 33636	6046 ± 49	4.71 ± 0.09	1.79 ± 0.19	-0.08 ± 0.06	3.2 ± 0.7	0.02 ± 0.11	[1]
HD 37124	5546 ± 30	4.50 ± 0.03	0.80 ± 0.07	-0.38 ± 0.04	4.5 ± 0.3	-0.07 ± 0.04	[1]
HD 39091	5991 ± 27	4.42 ± 0.10	1.24 ± 0.04	0.10 ± 0.04	4.9 ± 0.5	0.13 ± 0.07	[1]
HD 50554	6026 ± 30	4.41 ± 0.13	1.11 ± 0.06	0.01 ± 0.04	4.0 ± 0.4	0.01 ± 0.07	[1]
HD 65216	5666 ± 31	4.53 ± 0.09	1.06 ± 0.05	-0.12 ± 0.04	3.7 ± 0.5	-0.05 ± 0.08	[1]
HD 72659	5995 ± 45	4.30 ± 0.07	1.42 ± 0.09	0.03 ± 0.06	5.5 ± 0.5	0.11 ± 0.05	[1]
HD 73256	5518 ± 49	4.42 ± 0.12	1.22 ± 0.06	0.26 ± 0.06	4.8 ± 1.0	0.17 ± 0.12	[1]
HD 74156	6112 ± 39	4.34 ± 0.10	1.38 ± 0.07	0.16 ± 0.05	4.6 ± 0.3	0.11 ± 0.06	[1]
HD 106252	5899 ± 35	4.34 ± 0.07	1.08 ± 0.06	-0.01 ± 0.05	4.0 ± 0.8	-0.04 ± 0.11	[1]
HD 114729	5886 ± 36	4.28 ± 0.13	1.25 ± 0.09	-0.25 ± 0.05	4.9 ± 0.5	-0.06 ± 0.07	[1]
HD 213240	5984 ± 33	4.25 ± 0.10	1.25 ± 0.05	0.17 ± 0.05	5.7 ± 0.4	0.15 ± 0.06	[1]
HD 216435	5938 ± 42	4.12 ± 0.05	1.28 ± 0.06	0.24 ± 0.05	6.7 ± 0.7	0.18 ± 0.06	[1]
HD 216437	5887 ± 32	4.30 ± 0.07	1.31 ± 0.04	0.25 ± 0.04	6.2 ± 0.5	0.23 ± 0.05	[1]
BD 103166	5325 ± 45	4.36 ± 0.07	0.95 ± 0.05	0.35 ± 0.05	3.9 ± 1.0	0.06 ± 0.13	[3]
HD 2039	5976 ± 51	4.45 ± 0.10	1.26 ± 0.07	0.32 ± 0.06	4.2 ± 1.0	0.14 ± 0.12	[5]
HD 3651	5173 ± 35	4.37 ± 0.12	0.74 ± 0.05	0.12 ± 0.04	5.1 ± 0.5	0.12 ± 0.08	[4]
HD 4203	5636 ± 40	4.23 ± 0.14	1.12 ± 0.05	0.40 ± 0.05	3.8 ± 1.5	0.00 ± 0.21	[3]
HD 9826	6212 ± 64	4.26 ± 0.13	1.69 ± 0.16	0.13 ± 0.08	4.0 ± 0.7	0.02 ± 0.10	[2]
HD 16141	5801 ± 30	4.22 ± 0.12	1.34 ± 0.04	0.15 ± 0.04	4.7 ± 1.0	0.01 ± 0.11	[3]
HD 17051	6252 ± 53	4.61 ± 0.16	1.18 ± 0.10	0.26 ± 0.06	3.6 ± 0.7	0.16 ± 0.11	[1]
HD 19994	6190 ± 00	4.19 ± 0.00	1.54 ± 0.00	0.24 ± 0.00	5.0 ± 1.0	0.11 ± 0.09	[1]
HD 22049	5073 ± 42	4.43 ± 0.08	1.05 ± 0.06	-0.13 ± 0.05	3.8 ± 0.8	-0.07 ± 0.10	[2]
HD 23079	5959 ± 46	4.35 ± 0.12	1.20 ± 0.10	-0.11 ± 0.06	4.2 ± 0.2	-0.04 ± 0.06	[3]
HD 23596	6108 ± 36	4.25 ± 0.10	1.30 ± 0.05	0.31 ± 0.05	5.4 ± 0.3	0.18 ± 0.05	[2]
HD 27442	4825 ± 107	3.55 ± 0.32	1.18 ± 0.12	0.39 ± 0.13	15.6 ± 1.5	0.36 ± 0.16	[3]
HD 28185	5656 ± 44	4.45 ± 0.08	1.01 ± 0.06	0.22 ± 0.05	3.6 ± 1.0	0.02 ± 0.15	[5]
HD 30177	5587 ± 00	4.29 ± 0.00	1.08 ± 0.00	0.38 ± 0.00	3.3 ± 1.0	-0.04 ± 0.15	[5]
HD 38529	5674 ± 40	3.94 ± 0.12	1.38 ± 0.05	0.40 ± 0.06	13.3 ± 0.7	0.44 ± 0.06	[3]
HD 46375	5268 ± 55	4.41 ± 0.16	0.97 ± 0.06	0.20 ± 0.06	5.9 ± 0.5	0.23 ± 0.09	[2]
HD 50554	6026 ± 30	4.41 ± 0.13	1.11 ± 0.06	0.01 ± 0.04	5.3 ± 0.9	0.14 ± 0.09	[2]
HD 52265	6105 ± 00	4.28 ± 0.00	1.36 ± 0.00	0.23 ± 0.00	5.1 ± 0.7	0.14 ± 0.05	[3]
HD 59686	4871 ± 135	3.15 ± 0.24	1.85 ± 0.12	0.28 ± 0.18	33.8 ± 1.0	0.52 ± 0.13	[3]
HD 70642	5671 ± 46	4.39 ± 0.05	1.01 ± 0.06	0.20 ± 0.06	5.5 ± 0.5	0.17 ± 0.05	[3]
HD 73256	5518 ± 49	4.42 ± 0.12	1.22 ± 0.06	0.26 ± 0.06	3.5 ± 0.9	0.01 ± 0.14	[3]
HD 74156	6112 ± 39	4.34 ± 0.10	1.38 ± 0.07	0.16 ± 0.05	7.3 ± 0.7	0.31 ± 0.06	[3]
HD 75289	6143 ± 53	4.42 ± 0.13	1.53 ± 0.09	0.28 ± 0.07	5.6 ± 0.4	0.14 ± 0.08	[1]
HD 75732	5279 ± 62	4.37 ± 0.18	0.98 ± 0.07	0.33 ± 0.07	4.5 ± 0.7	0.13 ± 0.11	[2]
HD 82943	6015 ± 00	4.46 ± 0.00	1.13 ± 0.00	0.30 ± 0.00	4.8 ± 0.7	0.20 ± 0.06	[1]
HD 83443	5501 ± 63	4.46 ± 0.09	1.07 ± 0.08	0.39 ± 0.07	4.4 ± 1.0	0.17 ± 0.13	[3]
HD 92788	5758 ± 37	4.3 ± 0.04	1.1 ± 0.04	0.34 ± 0.05	3.8 ± 1.0	0.02 ± 0.13	[3]
HD 95128	5954 ± 25	4.44 ± 0.10	1.30 ± 0.04	0.06 ± 0.03	5.2 ± 0.6	0.15 ± 0.06	[4]
HD 106252	5834 ± 37	4.22 ± 0.02	1.06 ± 0.06	-0.03 ± 0.05	7.0 ± 1.0	0.14 ± 0.07	[3]
HD 108147	6248 ± 42	4.49 ± 0.16	1.35 ± 0.08	0.20 ± 0.05	3.7 ± 0.4	0.11 ± 0.09	[1]
HD 108874	5596 ± 42	4.37 ± 0.12	0.89 ± 0.05	0.23 ± 0.05	3.0 ± 0.7	-0.10 ± 0.12	[2]
HD 114386	4865 ± 93	4.3 ± 0.17	0.86 ± 0.12	-0.04 ± 0.07	5.1 ± 1.0	0.07 ± 0.15	[3]
HD 114762	5884 ± 34	4.22 ± 0.02	1.31 ± 0.17	-0.70 ± 0.04	3.2 ± 0.1	-0.36 ± 0.02	[1]
HD 114783	5098 ± 36	4.45 ± 0.11	0.74 ± 0.05	0.09 ± 0.04	4.4 ± 1.5	0.08 ± 0.18	[4]
HD 117176	5560 ± 34	4.07 ± 0.05	1.18 ± 0.05	-0.06 ± 0.05	7.1 ± 0.5	0.05 ± 0.04	[4]

The instruments used to obtain the spectra were: [1]UVES; [2]UES; [3]FEROS; [4]SARG; [5]CORALIE.

Table 4: Continued.

Star	T_{eff} (K)	$\log g$ (cm s^{-2})	ξ_t (km s^{-1})	[Fe/H]	$\text{EW}_{[\text{O I}]}$ (mÅ)	[O/H] _[\text{O I}]	Instr.
HD 121504	6075 ± 40	4.64 ± 0.12	1.31 ± 0.07	0.16 ± 0.05	3.5 ± 0.2	0.10 ± 0.06	[1]
HD 128311	4835 ± 72	4.44 ± 0.21	0.89 ± 0.11	0.03 ± 0.07	6.0 ± 1.5	0.19 ± 0.16	[2]
HD 134987	5776 ± 29	4.36 ± 0.07	1.09 ± 0.04	0.30 ± 0.04	6.5 ± 0.5	0.27 ± 0.05	[4]
HD 137759	4775 ± 113	3.09 ± 0.40	1.78 ± 0.11	0.13 ± 0.14	34.7 ± 1.0	0.48 ± 0.19	[4]
HD 141937	5909 ± 39	4.51 ± 0.08	1.13 ± 0.06	0.10 ± 0.05	4.6 ± 0.7	0.13 ± 0.07	[2]
HD 143761	5853 ± 25	4.41 ± 0.15	1.35 ± 0.07	-0.21 ± 0.04	4.5 ± 0.8	-0.02 ± 0.11	[4]
HD 145675	5311 ± 87	4.42 ± 0.18	0.92 ± 0.10	0.43 ± 0.08	5.7 ± 1.0	0.29 ± 0.12	[4]
HD 147513	5894 ± 31	4.43 ± 0.02	1.26 ± 0.05	0.08 ± 0.04	5.0 ± 1.5	0.12 ± 0.16	[3]
HD 150706	5961 ± 27	4.50 ± 0.10	1.11 ± 0.06	-0.01 ± 0.04	2.8 ± 0.5	-0.12 ± 0.09	[2]
HD 168443	5617 ± 35	4.22 ± 0.05	1.21 ± 0.05	0.06 ± 0.05	6.3 ± 1.0	0.11 ± 0.08	[4]
HD 168746	5601 ± 33	4.41 ± 0.12	0.99 ± 0.05	-0.08 ± 0.05	6.8 ± 0.5	0.19 ± 0.07	[4]
HD 177830	4804 ± 77	3.57 ± 0.17	1.14 ± 0.09	0.33 ± 0.09	16.0 ± 0.7	0.38 ± 0.09	[4]
HD 178911B	5600 ± 42	4.44 ± 0.08	0.95 ± 0.05	0.27 ± 0.05	5.9 ± 1.0	0.25 ± 0.08	[4]
HD 179949	6260 ± 43	4.43 ± 0.05	1.41 ± 0.09	0.22 ± 0.05	2.9 ± 1.0	-0.02 ± 0.18	[4]
HD 186427	5772 ± 25	4.40 ± 0.07	1.07 ± 0.04	0.08 ± 0.04	3.0 ± 0.3	-0.13 ± 0.05	[4]
HD 187123	5845 ± 22	4.42 ± 0.07	1.10 ± 0.03	0.13 ± 0.03	5.6 ± 0.5	0.18 ± 0.05	[4]
HD 190360	5584 ± 36	4.37 ± 0.06	1.07 ± 0.05	0.24 ± 0.05	6.1 ± 0.6	0.22 ± 0.04	[2]
HD 192263	4947 ± 58	4.51 ± 0.20	0.86 ± 0.09	-0.02 ± 0.06	4.1 ± 1.0	0.04 ± 0.15	[3]
HD 195019	5842 ± 31	4.32 ± 0.07	1.27 ± 0.05	0.09 ± 0.04	3.7 ± 0.7	-0.07 ± 0.09	[2]
HD 209458	6117 ± 26	4.48 ± 0.08	1.40 ± 0.06	0.02 ± 0.03	4.0 ± 0.8	0.06 ± 0.10	[1]
HD 210277	5532 ± 00	4.29 ± 0.00	1.03 ± 0.00	0.19 ± 0.00	6.6 ± 0.5	0.21 ± 0.04	[4]
HD 213240	5984 ± 33	4.25 ± 0.10	1.25 ± 0.05	0.17 ± 0.05	9.0 ± 1.5	0.35 ± 0.09	[5]
HD 216770	5423 ± 41	4.40 ± 0.13	1.01 ± 0.05	0.26 ± 0.04	10.2 ± 2.0	0.49 ± 0.12	[4]
HD 217014	5804 ± 36	4.42 ± 0.07	1.20 ± 0.05	0.20 ± 0.05	5.4 ± 1.0	0.19 ± 0.11	[3]
HD 217107	5645 ± 00	4.31 ± 0.00	1.06 ± 0.00	0.37 ± 0.00	5.4 ± 0.2	0.18 ± 0.01	[2]
HD 222582	5843 ± 38	4.45 ± 0.07	1.03 ± 0.06	0.05 ± 0.05	4.8 ± 1.0	0.10 ± 0.11	[2]
HD 104985	4773 ± 62	2.76 ± 0.14	1.71 ± 0.07	-0.28 ± 0.09	42.7 ± 1.5	0.30 ± 0.07^1	[4]

The instruments used to obtain the spectra were: [1]UVES; [2]UES; [3]FEROS; [4]SARG; [5]CORALIE.

¹ This value was excluded from the figures since it is inconsistent with the triplet result.

Table 5: Oxygen abundances from [O I] line in a set of comparison stars.

Star	T_{eff} (K)	$\log g$ (cm s^{-2})	ξ_t (km s^{-1})	[Fe/H]	$\text{EW}_{[\text{O I}]}$ (mÅ)	[O/H] _[\text{O I}]	Instr.
HD 1581	5956 ± 44	4.39 ± 0.13	1.07 ± 0.09	-0.14 ± 0.05	4.8 ± 0.2	0.03 ± 0.07	[3]
HD 7570	6140 ± 41	4.39 ± 0.16	1.50 ± 0.08	0.18 ± 0.05	3.8 ± 0.3	0.05 ± 0.09	[1]
HD 52919	4740 ± 49	4.25 ± 0.1	1.03 ± 0.09	-0.05 ± 0.06	4.8 ± 1.0	-0.04 ± 0.11	[3]
HD 53143	5462 ± 54	4.47 ± 0.07	1.08 ± 0.07	0.22 ± 0.06	1.9 ± 0.5	-0.25 ± 0.14	[3]
HD 67199	5136 ± 56	4.54 ± 0.08	0.84 ± 0.08	0.06 ± 0.06	6.3 ± 2.0	0.28 ± 0.18	[3]
HD 100623	5246 ± 37	4.54 ± 0.05	1 ± 0.06	-0.38 ± 0.05	2.3 ± 0.5	-0.32 ± 0.10	[3]
HD 102365	5667 ± 27	4.59 ± 0.02	1.05 ± 0.06	-0.27 ± 0.04	3.8 ± 0.5	-0.04 ± 0.07	[3]
HD 104304	5562 ± 50	4.37 ± 0.06	1.1 ± 0.06	0.27 ± 0.06	6.0 ± 0.5	0.22 ± 0.05	[3]
HD 109200	5103 ± 46	4.47 ± 0.07	0.75 ± 0.07	-0.24 ± 0.05	5.2 ± 0.4	0.06 ± 0.05	[3]
HD 115617	5577 ± 33	4.34 ± 0.03	1.07 ± 0.04	0.01 ± 0.05	4.6 ± 1.0	0.00 ± 0.11	[3]
HD 118972	5241 ± 66	4.43 ± 0.1	1.24 ± 0.08	-0.01 ± 0.08	3.6 ± 0.9	-0.06 ± 0.19	[3]
HD 125072	5001 ± 115	4.39 ± 0.21	1.21 ± 0.15	0.24 ± 0.11	8.3 ± 1.0	0.39 ± 0.12	[3]
HD 140901	5645 ± 37	4.4 ± 0.04	1.14 ± 0.05	0.13 ± 0.05	6.2 ± 1.5	0.21 ± 0.12	[3]
HD 144628	5071 ± 43	4.41 ± 0.06	0.82 ± 0.07	-0.36 ± 0.06	6.5 ± 0.8	0.09 ± 0.07	[3]
HD 146233	5786 ± 35	4.31 ± 0.03	1.18 ± 0.05	0.08 ± 0.05	7.7 ± 1.0	0.26 ± 0.07	[3]
HD 152391	5521 ± 43	4.54 ± 0.05	1.29 ± 0.06	0.03 ± 0.05	4.7 ± 0.7	0.12 ± 0.08	[3]

The instruments used to obtain the spectra were: [1]UVES; [2]UES; [3]FEROS; [4]SARG; [5]CORALIE.

Table 5: Continued.

Star	T_{eff} (K)	$\log g$ (cm s^{-2})	ξ_t (km s^{-1})	[Fe/H]	$\text{EW}_{[\text{O I}]}$ (mÅ)	$[\text{O}/\text{H}]_{[\text{O I}]}$	Instr.
HD 154088	5414 ± 60	4.28 ± 0.08	1.14 ± 0.07	0.33 ± 0.07	6.6 ± 0.7	0.25 ± 0.07	[3]
HD 156274	5300 ± 32	4.41 ± 0.04	1 ± 0.05	-0.33 ± 0.05	5.0 ± 0.9	-0.02 ± 0.09	[3]
HD 165499	5950 ± 45	4.31 ± 0.02	1.14 ± 0.08	0.01 ± 0.06	4.5 ± 1.0	0.01 ± 0.10	[3]
HD 170657	5115 ± 52	4.48 ± 0.08	1.13 ± 0.07	-0.22 ± 0.06	4.0 ± 0.5	-0.05 ± 0.07	[3]
HD 172051	5634 ± 30	4.43 ± 0.03	1.06 ± 0.05	-0.20 ± 0.04	4.7 ± 0.5	-0.01 ± 0.05	[3]
HD 177565	5664 ± 28	4.43 ± 0.02	1.02 ± 0.04	0.14 ± 0.04	6.2 ± 0.5	0.23 ± 0.04	[3]
HD 192310	5069 ± 49	4.38 ± 0.19	0.79 ± 0.07	-0.01 ± 0.05	4.5 ± 0.5	0.03 ± 0.11	[4]
HD 222335	5260 ± 41	4.45 ± 0.11	0.92 ± 0.06	-0.16 ± 0.05	8.0 ± 1.0	0.27 ± 0.07	[3]

The instruments used to obtain the spectra were: [1]UVES; [2]UES; [3]FEROS; [4]SARG; [5]CORALIE.

¹ This value was excluded from the figures since it is inconsistent with the triplet result.

Table 6: Oxygen abundances from OH band synthesis for a set of stars with planets and brown dwarf companions.

Star	T_{eff} (K)	$\log g$ (cm s^{-2})	ξ_t (km s^{-1})	[Fe/H]	$[\text{O}/\text{H}]_1$	$[\text{O}/\text{H}]_2$	$[\text{O}/\text{H}]_3$	$[\text{O}/\text{H}]_4$	$[\text{O}/\text{H}]_{\text{avg}}$
HD 142	6302 ± 56	4.34 ± 0.13	1.86 ± 0.17	0.14 ± 0.07	-0.02	0.03	0.08	0.18	0.07 ± 0.13
HD 1237	5536 ± 50	4.56 ± 0.12	1.33 ± 0.06	0.12 ± 0.06	0.06	0.01	0.06	0.16	0.07 ± 0.10
HD 4208	5626 ± 32	4.49 ± 0.10	0.95 ± 0.06	-0.24 ± 0.04	-0.15	-0.10	-0.20	-0.10	-0.14 ± 0.08
HD 23079	5959 ± 46	4.35 ± 0.12	1.20 ± 0.10	-0.11 ± 0.06	-0.02	0.03	0.03	0.03	0.02 ± 0.09
HD 28185	5656 ± 44	4.45 ± 0.08	1.01 ± 0.06	0.22 ± 0.05	0.16	0.26	0.21	0.31	0.23 ± 0.10
HD 30177	5591 ± 50	4.35 ± 0.12	1.03 ± 0.06	0.39 ± 0.06	0.23	0.23	0.38	0.38	0.31 ± 0.12
HD 33636	6046 ± 49	4.71 ± 0.09	1.79 ± 0.19	-0.08 ± 0.06	0.01	0.06	0.11	0.11	0.07 ± 0.10
HD 37124	5546 ± 30	4.50 ± 0.03	0.80 ± 0.07	-0.38 ± 0.04	-0.14	-0.04	-0.04	-0.04	-0.06 ± 0.08
HD 39091	5991 ± 27	4.42 ± 0.10	1.24 ± 0.04	0.10 ± 0.04	0.19	0.19	0.24	0.29	0.23 ± 0.08
HD 47536	4554 ± 85	2.48 ± 0.23	1.82 ± 0.08	-0.54 ± 0.12	-0.30	-0.30	-0.20	-0.35	-0.29 ± 0.12
HD 50554	6026 ± 30	4.41 ± 0.13	1.11 ± 0.06	0.01 ± 0.04	0.15	0.15	0.15	0.25	0.17 ± 0.09
HD 59686	4871 ± 135	3.15 ± 0.41	1.85 ± 0.12	0.28 ± 0.18	0.12	0.12	0.22	0.12	0.14 ± 0.16
HD 65216	5666 ± 31	4.53 ± 0.09	1.06 ± 0.05	-0.12 ± 0.04	-0.08	0.02	0.02	0.02	-0.00 ± 0.08
HD 70642	5693 ± 26	4.41 ± 0.09	1.01 ± 0.04	0.18 ± 0.04	0.12	0.12	0.22	0.22	0.17 ± 0.09
HD 72659	5995 ± 45	4.30 ± 0.07	1.42 ± 0.09	0.03 ± 0.06	0.17	0.17	0.22	0.27	0.21 ± 0.09
HD 73256	5518 ± 49	4.42 ± 0.12	1.22 ± 0.06	0.26 ± 0.06	0.00	0.10	0.15	0.20	0.11 ± 0.11
HD 74156	6112 ± 39	4.34 ± 0.10	1.38 ± 0.07	0.16 ± 0.05	0.30	0.30	0.35	0.35	0.32 ± 0.08
HD 88133	5438 ± 34	3.94 ± 0.11	1.16 ± 0.03	0.33 ± 0.05	0.17	0.17	0.27	0.27	0.22 ± 0.09
HD 99492	4810 ± 72	4.21 ± 0.21	0.72 ± 0.13	0.26 ± 0.07	0.00	0.00	0.05	0.00	0.01 ± 0.08
HD 106252	5899 ± 35	4.34 ± 0.07	1.08 ± 0.06	-0.01 ± 0.05	0.08	0.08	0.13	0.08	0.09 ± 0.07
HD 114729	5886 ± 36	4.28 ± 0.13	1.25 ± 0.09	-0.25 ± 0.05	-0.01	-0.01	-0.01	-0.01	-0.01 ± 0.07
HD 117207	5654 ± 33	4.32 ± 0.05	1.13 ± 0.04	0.23 ± 0.05	0.12	0.17	0.22	0.27	0.19 ± 0.09
HD 117618	6013 ± 41	4.39 ± 0.07	1.73 ± 0.09	0.06 ± 0.06	0.12	0.10	0.15	0.20	0.14 ± 0.09
HD 213240	5984 ± 33	4.25 ± 0.10	1.25 ± 0.05	0.17 ± 0.05	0.23	0.21	0.26	0.31	0.25 ± 0.08
HD 216435	5938 ± 42	4.12 ± 0.05	1.28 ± 0.06	0.24 ± 0.05	0.20	0.13	0.28	0.33	0.23 ± 0.12
HD 216437	5887 ± 32	4.30 ± 0.07	1.31 ± 0.04	0.25 ± 0.04	0.20	0.13	0.28	0.28	0.22 ± 0.10
HD 219449	4757 ± 102	2.71 ± 0.25	1.71 ± 0.09	0.05 ± 0.14	-0.16	-0.11	-0.01	-0.11	-0.10 ± 0.13
HD 6434	5835 ± 50	4.60 ± 0.15	1.53 ± 0.10	-0.52 ± 0.05	-0.26	-0.13	-0.20	-0.13	-0.18 ± 0.10
HD 9826	6212 ± 64	4.26 ± 0.13	1.69 ± 0.16	0.13 ± 0.08	0.17	0.27	0.17	0.27	0.22 ± 0.12
HD 10647	6143 ± 31	4.48 ± 0.08	1.40 ± 0.08	-0.03 ± 0.04	-0.01	-0.11	-0.01	-0.11	-0.06 ± 0.09
HD 13445	5163 ± 37	4.52 ± 0.13	0.72 ± 0.06	-0.24 ± 0.05	-0.40	-0.20	-0.20	-0.20	-0.25 ± 0.12
HD 16141	5801 ± 30	4.22 ± 0.12	1.34 ± 0.04	0.15 ± 0.04	0.09	0.24	0.25	0.20	0.19 ± 0.10
HD 17051	6252 ± 53	4.61 ± 0.16	1.18 ± 0.10	0.26 ± 0.06	0.29	0.34	0.39	0.29	0.33 ± 0.11
HD 19994	6190 ± 57	4.19 ± 0.13	1.54 ± 0.13	0.24 ± 0.07	0.28	0.33	0.38	0.23	0.31 ± 0.12
HD 22049	5073 ± 42	4.43 ± 0.08	1.05 ± 0.06	-0.13 ± 0.04	-0.34	-0.18	-0.22	-0.19	-0.23 ± 0.10

Table 6: Continued.

Star	T_{eff} (K)	$\log g$ (cm s^{-2})	ξ_t (km s^{-1})	[Fe/H]	[O/H] ₁	[O/H] ₂	[O/H] ₃	[O/H] ₄	[O/H] _{avg}
HD 27442	4825 ± 107	3.55 ± 0.32	1.18 ± 0.12	0.39 ± 0.13	-0.02	0.16	0.08	-	0.07 ± 0.14
HD 46375	5268 ± 55	4.41 ± 0.16	0.97 ± 0.06	0.20 ± 0.06	-0.06	0.09	0.09	0.04	0.04 ± 0.10
HD 52265	6103 ± 52	4.28 ± 0.15	1.36 ± 0.09	0.23 ± 0.07	0.19	0.19	0.27	0.19	0.21 ± 0.10
HD 75289	6143 ± 53	4.42 ± 0.13	1.53 ± 0.09	0.28 ± 0.07	0.19	0.19	0.29	0.19	0.22 ± 0.11
HD 82943	6016 ± 30	4.46 ± 0.08	1.13 ± 0.04	0.30 ± 0.04	0.24	0.29	0.39	0.24	0.29 ± 0.10
HD 83443	5454 ± 61	4.33 ± 0.17	1.08 ± 0.08	0.35 ± 0.08	-0.01	0.19	0.19	-	0.12 ± 0.13
HD 143761	5853 ± 25	4.41 ± 0.15	1.35 ± 0.07	-0.21 ± 0.04	-0.17	-0.07	-0.07	-0.07	-0.09 ± 0.08
HD 169830	6299 ± 41	4.10 ± 0.02	1.42 ± 0.09	0.21 ± 0.05	0.19	0.29	0.29	0.09	0.22 ± 0.12
HD 179949	6260 ± 43	4.43 ± 0.05	1.41 ± 0.09	0.22 ± 0.05	0.22	0.34	0.29	0.19	0.26 ± 0.11
HD 192263	4947 ± 58	4.51 ± 0.20	0.86 ± 0.09	-0.02 ± 0.06	-0.21	-0.11	-0.18	-0.16	-0.17 ± 0.09
HD 202206	5752 ± 53	4.50 ± 0.09	1.01 ± 0.06	0.35 ± 0.06	0.14	0.24	0.24	0.19	0.20 ± 0.09
HD 209458	6117 ± 26	4.48 ± 0.08	1.40 ± 0.06	0.02 ± 0.03	-0.01	0.06	0.06	0.02	0.03 ± 0.07
HD 210277	5532 ± 28	4.29 ± 0.09	1.04 ± 0.03	0.19 ± 0.04	-0.01	0.19	0.22	0.11	0.13 ± 0.12
HD 217014	5804 ± 36	4.42 ± 0.07	1.20 ± 0.05	0.20 ± 0.05	0.04	-0.11	-0.01	-0.16	-0.06 ± 0.11
HD 217107	5646 ± 34	4.31 ± 0.10	1.06 ± 0.04	0.37 ± 0.05	0.14	0.34	0.39	0.29	0.29 ± 0.13
HD 222582	5843 ± 38	4.45 ± 0.07	1.03 ± 0.06	0.05 ± 0.05	0.04	0.14	0.09	0.09	0.09 ± 0.08

Table 7: Oxygen abundances from OH band synthesis for a set of comparison stars (stars without giant planets).

Star	T_{eff} (K)	$\log g$ (cm s^{-2})	ξ_t (km s^{-1})	[Fe/H]	[O/H] ₁	[O/H] ₂	[O/H] ₃	[O/H] ₄	[O/H] _{avg}
HD 1461	5785 ± 50	4.47 ± 0.15	1.00 ± 0.10	0.18 ± 0.05	0.09	0.19	0.24	0.19	0.18 ± 0.10
HD 1581	5956 ± 44	4.39 ± 0.13	1.07 ± 0.09	-0.14 ± 0.05	-0.05	0.00	0.05	0.00	0.00 ± 0.09
HD 3823	5950 ± 50	4.12 ± 0.15	1.00 ± 0.10	-0.27 ± 0.05	-0.13	-0.05	-0.05	-0.08	-0.08 ± 0.09
HD 4391	5878 ± 53	4.74 ± 0.15	1.13 ± 0.10	-0.03 ± 0.06	-0.09	0.04	0.03	0.00	-0.00 ± 0.10
HD 7570	6140 ± 41	4.39 ± 0.16	1.50 ± 0.08	0.18 ± 0.05	0.22	0.27	0.32	0.22	0.26 ± 0.09
HD 10700	5344 ± 29	4.57 ± 0.09	0.91 ± 0.06	-0.52 ± 0.04	-0.48	-0.28	-0.38	-0.38	-0.38 ± 0.10
HD 14412	5368 ± 24	4.55 ± 0.05	0.88 ± 0.05	-0.47 ± 0.03	-0.53	-0.33	-0.43	-0.33	-0.41 ± 0.11
HD 20010	6275 ± 57	4.40 ± 0.37	2.41 ± 0.41	-0.19 ± 0.06	-0.08	-0.07	0.00	-0.05	-0.05 ± 0.12
HD 20766	5733 ± 31	4.55 ± 0.10	1.09 ± 0.06	-0.21 ± 0.04	-0.17	-0.07	-0.12	-0.07	-0.11 ± 0.08
HD 20794	5444 ± 31	4.47 ± 0.07	0.98 ± 0.06	-0.38 ± 0.04	-0.24	-0.04	-0.14	-0.04	-0.12 ± 0.11
HD 20807	5843 ± 26	4.47 ± 0.10	1.17 ± 0.06	-0.23 ± 0.04	-0.12	-0.06	-0.09	-0.09	-0.09 ± 0.07
HD 23484	5176 ± 45	4.41 ± 0.17	1.03 ± 0.06	0.06 ± 0.05	-0.27	-0.09	-0.10	-0.13	-0.15 ± 0.11
HD 30495	5868 ± 30	4.55 ± 0.10	1.24 ± 0.05	0.02 ± 0.04	-0.04	0.11	0.06	0.01	0.04 ± 0.09
HD 36435	5479 ± 37	4.61 ± 0.07	1.12 ± 0.05	-0.00 ± 0.05	-0.26	-0.11	-0.11	-0.16	-0.16 ± 0.10
HD 38858	5752 ± 32	4.53 ± 0.07	1.26 ± 0.07	-0.23 ± 0.05	-0.19	-0.09	-0.14	-0.14	-0.14 ± 0.08
HD 43162	5633 ± 35	4.48 ± 0.07	1.24 ± 0.05	-0.01 ± 0.04	-0.20	-0.07	-0.07	-0.17	-0.13 ± 0.09
HD 43834	5594 ± 36	4.41 ± 0.09	1.05 ± 0.04	0.10 ± 0.05	0.00	0.14	0.14	0.09	0.09 ± 0.10
HD 69830	5410 ± 26	4.38 ± 0.07	0.89 ± 0.03	-0.03 ± 0.04	-0.09	0.06	0.01	0.01	-0.00 ± 0.09
HD 72673	5242 ± 28	4.50 ± 0.09	0.69 ± 0.05	-0.37 ± 0.04	-0.43	-0.23	-0.33	-0.23	-0.31 ± 0.11
HD 74576	5000 ± 55	4.55 ± 0.13	1.07 ± 0.08	-0.03 ± 0.06	-0.34	-0.19	-0.22	-0.24	-0.25 ± 0.10
HD 76151	5803 ± 29	4.50 ± 0.08	1.02 ± 0.04	0.14 ± 0.04	0.13	0.26	0.23	0.18	0.20 ± 0.09
HD 84117	6167 ± 37	4.35 ± 0.10	1.42 ± 0.09	-0.03 ± 0.05	0.04	0.11	0.11	0.01	0.07 ± 0.09
HD 189567	5765 ± 24	4.52 ± 0.05	1.22 ± 0.05	-0.23 ± 0.04	-0.09	0.06	-0.04	0.01	-0.01 ± 0.09
HD 192310	5069 ± 49	4.38 ± 0.19	0.79 ± 0.07	-0.01 ± 0.05	-0.27	-0.07	-0.17	-0.12	-0.16 ± 0.11
HD 211415	5890 ± 30	4.51 ± 0.07	1.12 ± 0.07	-0.17 ± 0.04	-0.03	0.00	-0.08	-0.03	-0.04 ± 0.07
HD 222335	5260 ± 41	4.45 ± 0.11	0.92 ± 0.06	-0.16 ± 0.05	-0.32	-0.17	-0.10	-0.17	-0.19 ± 0.12

Table 8: Oxygen abundances from Triplet lines in a set of planet host stars.

Star	T_{eff} (K)	$\log g$ (cm s^{-2})	ξ_t (km s^{-1})	[Fe/H]	EW ₁ (mÅ)	[O/H] ₁ 7775 Å	[O/H] ₁ ^{NLTE} 7775 Å	EW ₂ (mÅ)	[O/H] ₂ 7774 Å	[O/H] ₂ ^{NLTE} 7774 Å	EW ₃ (mÅ)	[O/H] ₃ 7772 Å	[O/H] ₃ ^{NLTE} 7772 Å	[O/H] _{avg} ^{NLTE}	Instr.
HD 3651	5173 ± 35	4.37 ± 0.12	0.74 ± 0.05	0.12 ± 0.04	44.7	0.21	0.00	42.8	0.31	0.11	33.4	0.31	0.14	0.08 ± 0.10	[4]
HD 8574	6151 ± 57	4.51 ± 0.10	1.45 ± 0.15	0.06 ± 0.07	121.0	0.22	-0.26	100.2	0.15	-0.26	80.5	0.12	-0.29	-0.27 ± 0.08	[4]
HD 9826	6212 ± 64	4.26 ± 0.13	1.69 ± 0.16	0.13 ± 0.08	125.9	0.18	-0.33	112.0	0.18	-0.28	94.0	0.18	-0.21	-0.27 ± 0.09	[2]
HD 10697	5641 ± 28	4.05 ± 0.05	1.13 ± 0.03	0.14 ± 0.04	118.7	0.61	0.13	90.2	0.43	0.04	81.1	0.52	0.13	0.10 ± 0.08	[4]
HD 12661	5702 ± 36	4.33 ± 0.08	1.05 ± 0.04	0.36 ± 0.05	82.3	0.20	-0.13	70.5	0.18	-0.10	56.6	0.16	-0.07	-0.10 ± 0.07	[2]
HD 16141	5801 ± 30	4.22 ± 0.12	1.34 ± 0.04	0.15 ± 0.04	83.0	0.04	-0.32	74.3	0.07	-0.26	60.8	0.07	-0.20	-0.26 ± 0.08	[2]
HD 19994	6190 ± 00	4.19 ± 0.00	1.54 ± 0.00	0.24 ± 0.00	133.5	0.29	-0.24	123.4	0.34	-0.15	92.0	0.17	-0.20	-0.20 ± 0.07	[2]
HD 22049	5073 ± 42	4.43 ± 0.08	1.05 ± 0.06	-0.13 ± 0.05	26.5	-0.12	-0.28	24.2	-0.04	-0.19	15.6	-0.14	-0.26	-0.24 ± 0.10	[2]
HD 23596	6108 ± 36	4.25 ± 0.10	1.30 ± 0.05	0.31 ± 0.05	117.8	0.23	-0.23	105.1	0.23	-0.18	85.2	0.19	-0.14	-0.18 ± 0.08	[2]
HD 37124	5546 ± 30	4.50 ± 0.03	0.80 ± 0.07	-0.38 ± 0.04	69.2	0.14	-0.16	58.2	0.13	-0.14	43.6	0.11	-0.11	-0.14 ± 0.07	[2]
HD 40979	6145 ± 42	4.31 ± 0.15	1.29 ± 0.09	0.21 ± 0.05	122.5	0.25	-0.23	111.4	0.28	-0.16	88.0	0.21	-0.14	-0.18 ± 0.08	[4]
HD 46375	5268 ± 55	4.41 ± 0.16	0.97 ± 0.06	0.20 ± 0.06	51.2	0.22	-0.01	48.3	0.31	0.09	40.5	0.37	0.18	0.09 ± 0.14	[2]
HD 50554	6026 ± 30	4.41 ± 0.13	1.11 ± 0.06	0.01 ± 0.04	88.6	-0.04	-0.42	81.1	0.01	-0.34	64.6	0.00	-0.29	-0.35 ± 0.10	[2]
HD 59686	4871 ± 135	3.15 ± 0.24	1.85 ± 0.12	0.28 ± 0.18	47.3	0.27	0.01	48.0	0.43	0.17	40.2	0.46	0.23	0.14 ± 0.30	[3]
HD 68988	5988 ± 52	4.45 ± 0.15	1.25 ± 0.08	0.36 ± 0.06	105.8	0.23	-0.16	92.5	0.22	-0.12	75.5	0.21	-0.07	-0.12 ± 0.10	[4]
HD 70642	5671 ± 46	4.39 ± 0.05	1.01 ± 0.06	0.20 ± 0.06	80.3	0.20	-0.13	68.9	0.18	-0.11	64.0	0.33	0.06	-0.06 ± 0.13	[3]
HD 73256	5518 ± 49	4.42 ± 0.12	1.22 ± 0.06	0.26 ± 0.06	68.3	0.22	-0.06	59.2	0.22	-0.03	44.6	0.17	-0.03	-0.04 ± 0.08	[3]
HD 75732	5279 ± 62	4.37 ± 0.18	0.98 ± 0.07	0.33 ± 0.07	51.7	0.22	0.00	47.1	0.28	0.07	33.7	0.19	0.03	0.03 ± 0.11	[2]
HD 80606	5574 ± 72	4.46 ± 0.20	1.14 ± 0.09	0.32 ± 0.09	71.9	0.20	-0.09	61.8	0.19	-0.06	51.1	0.23	0.02	-0.04 ± 0.13	[2]
HD 82943	6015 ± 00	4.46 ± 0.00	1.13 ± 0.00	0.30 ± 0.00	103.4	0.18	-0.21	87.1	0.13	-0.20	74.3	0.18	-0.10	-0.17 ± 0.08	[2]
HD 83443	5501 ± 63	4.46 ± 0.09	1.07 ± 0.08	0.39 ± 0.07	85.9	0.49	0.17	73.8	0.48	0.20	53.5	0.37	0.16	0.17 ± 0.09	[3]
HD 89744	6234 ± 45	3.98 ± 0.05	1.62 ± 0.08	0.22 ± 0.05	140.2	0.30	-0.29	124.8	0.27	-0.26	101.0	0.20	-0.23	-0.26 ± 0.07	[2]
HD 92788	5758 ± 37	4.30 ± 0.04	1.10 ± 0.04	0.34 ± 0.05	95.3	0.99	0.62	72.7	0.93	0.63	67.3	1.03	0.76	0.67 ± 0.09 ¹	[3]
HD 104985	4773 ± 62	2.76 ± 0.14	1.71 ± 0.07	-0.28 ± 0.09	54.7	-0.19	-0.48	50.3	-0.12	-0.38	40.1	-0.11	-0.33	-0.40 ± 0.20	[4]
HD 106252	5834 ± 37	4.22 ± 0.02	1.06 ± 0.06	-0.03 ± 0.05	84.7	0.04	-0.34	72.9	0.02	-0.32	57.8	0.01	-0.27	-0.31 ± 0.07	[3]
HD 108874	5596 ± 42	4.37 ± 0.12	0.89 ± 0.05	0.23 ± 0.05	64.2	0.05	-0.23	58.5	0.10	-0.16	44.1	0.05	-0.15	-0.18 ± 0.08	[2]
HD 114386	4865 ± 93	4.30 ± 0.17	0.86 ± 0.12	-0.04 ± 0.07	37.8	1.27	1.10	24.9	1.20	1.06	-	-	-	1.15 ± 0.18 ¹	[3]
HD 114762	5884 ± 34	4.22 ± 0.02	1.31 ± 0.17	-0.70 ± 0.04	65.1	-0.31	-0.64	53.2	-0.34	-0.63	42.0	-0.31	-0.55	-0.61 ± 0.08	[2]
HD 117176	5560 ± 34	4.07 ± 0.05	1.18 ± 0.05	-0.06 ± 0.05	70.0	0.06	-0.28	56.3	-0.02	-0.31	40.2	-0.11	-0.33	-0.31 ± 0.07	[4]
HD 120136	6339 ± 73	4.19 ± 0.10	1.70 ± 0.16	0.23 ± 0.07	166.2	0.49	-0.16	140.8	0.40	-0.16	118.1	0.37	-0.10	-0.14 ± 0.08	[2]
HD 130322	5392 ± 36	4.48 ± 0.06	0.85 ± 0.05	0.03 ± 0.04	51.5	0.06	-0.18	47.6	0.14	-0.09	37.4	0.15	-0.04	-0.10 ± 0.10	[4]
HD 134987	5776 ± 29	4.36 ± 0.07	1.09 ± 0.04	0.30 ± 0.04	101.2	0.36	-0.03	85.4	0.31	-0.03	75.0	0.39	0.10	0.01 ± 0.10	[4]
HD 136118	6222 ± 39	4.27 ± 0.15	1.79 ± 0.12	-0.04 ± 0.05	145.0	0.34	-0.27	121.5	0.25	-0.28	90.5	0.11	-0.29	-0.28 ± 0.06	[4]
HD 141937	5909 ± 39	4.51 ± 0.08	1.13 ± 0.06	0.10 ± 0.05	90.3	0.10	-0.27	83.6	0.17	-0.17	63.6	0.10	-0.17	-0.20 ± 0.09	[2]
HD 143761	5853 ± 25	4.41 ± 0.15	1.35 ± 0.07	-0.21 ± 0.04	74.0	-0.12	-0.46	66.2	-0.08	-0.39	52.8	-0.07	-0.33	-0.39 ± 0.10	[4]
HD 147513	5894 ± 31	4.43 ± 0.02	1.26 ± 0.05	0.08 ± 0.04	90.6	0.09	-0.28	71.9	0.01	-0.30	64.8	0.11	-0.17	-0.25 ± 0.09	[3]
HD 150706	5961 ± 27	4.50 ± 0.10	1.11 ± 0.06	-0.01 ± 0.04	80.3	-0.08	-0.43	70.1	-0.07	-0.38	50.1	-0.16	-0.39	-0.40 ± 0.07	[2]
HD 168443	5617 ± 35	4.22 ± 0.05	1.21 ± 0.05	0.06 ± 0.05	68.5	0.02	-0.30	54.8	0.06	-0.33	45.3	0.02	-0.25	-0.29 ± 0.07	[4]
HD 168746	5601 ± 33	4.41 ± 0.12	0.99 ± 0.05	-0.08 ± 0.05	73.2	0.14	-0.19	64.6	0.17	-0.13	49.8	0.14	-0.10	-0.14 ± 0.08	[4]
HD 178911B	5600 ± 42	4.44 ± 0.08	0.95 ± 0.05	0.27 ± 0.05	79.2	0.28	-0.03	72.0	0.33	0.04	62.6	0.40	0.15	0.05 ± 0.12	[4]
HD 179949	6260 ± 43	4.43 ± 0.05	1.41 ± 0.09	0.23 ± 0.05	130.9	0.26	-0.23	115.6	0.25	-0.19	91.3	0.18	-0.17	-0.20 ± 0.07	[4]
HD 186427	5772 ± 25	4.40 ± 0.07	1.07 ± 0.04	0.08 ± 0.04	73.7	-0.01	-0.33	67.4	0.05	-0.25	53.2	0.04	-0.20	-0.26 ± 0.09	[4]
HD 187123	5845 ± 22	4.42 ± 0.07	1.10 ± 0.03	0.13 ± 0.03	82.6	0.05	-0.29	70.0	0.02	-0.28	56.1	0.02	-0.22	-0.26 ± 0.07	[4]
HD 190228	5325 ± 00	3.90 ± 0.00	1.11 ± 0.00	-0.26 ± 0.00	43.9	-0.19	-0.44	34.4	-0.25	-0.47	30.4	-0.14	-0.34	-0.42 ± 0.09	[2]
HD 190360	5584 ± 36	4.37 ± 0.06	1.07 ± 0.05	0.24 ± 0.05	78.6	0.26	-0.06	67.6	0.25	-0.03	57.0	0.30	0.06	-0.01 ± 0.09	[2]
HD 192263	4947 ± 58	4.51 ± 0.20	0.86 ± 0.09	-0.02 ± 0.06	30.2	0.21	0.05	23.0	0.14	0.01	20.0	0.25	0.13	0.06 ± 0.12	[3]
HD 195019	5859 ± 31	4.32 ± 0.07	1.27 ± 0.05	0.09 ± 0.04	83.0	0.01	-0.35	72.0	0.00	-0.32	55.3	-0.04	-0.29	-0.32 ± 0.07	[2]
HD 210277	5532 ± 00	4.29 ± 0.00	1.03 ± 0.00	0.19 ± 0.00	76.6	0.27	-0.05	65.2	0.25	-0.03	53.1	0.26	0.02	-0.02 ± 0.06	[2]
HD 216770	5423 ± 41	4.40 ± 0.13	1.01 ± 0.05	0.26 ± 0.04	57.0	0.13	-0.12	53.5	0.21	-0.02	40.1	0.16	-0.02	-0.05 ± 0.10	[4]
HD 217107	5645 ± 00	4.31 ± 0.00	1.06 ± 0.00	0.37 ± 0.00	73.8	0.13	-0.17	69.7	0.22	-0.06	55.3	0.20	-0.03	-0.09 ± 0.09	[2]
HD 219542B	5732 ± 31	4.40 ± 0.05	0.99 ± 0.04	0.17 ± 0.04	85.3	0.20	-0.15	73.5	0.19	-0.12	52.0	0.06	-0.17	-0.15 ± 0.07	[4]
HD 222582	5843 ± 38	4.45 ± 0.07	1.03 ± 0.06	0.05 ± 0.05	79.2	0.12	-0.22	70.1	0.14	-0.17	53.9	0.10	-0.14	-0.18 ± 0.08	[2]
BD 103166	5325 ± 45	4.36 ± 0.07	0.95 ± 0.05	0.35 ± 0.05	66.2	0.41	0.14	61.3	0.48	0.23	41.0	0.31	0.13	0.17 ± 0.09	[3]

The instruments used to obtain the spectra were: [1]UVES; [2]UES; [3]FEROS; [4]SARG; [5]CORALIE.

Table 9: Oxygen abundances from Triplet lines in a set of comparison stars.

Star	T_{eff} (K)	$\log g$ (cm s^{-2})	ξ_t (km s^{-1})	[Fe/H]	EW ₁ (mÅ)	[O/H] ₁ 7775 Å	[O/H] ₁ ^{NLTE} 7775 Å	EW ₂ (mÅ)	[O/H] ₂ 7774 Å	[O/H] ₂ ^{NLTE} 7774 Å	EW ₃ (mÅ)	[O/H] ₃ 7772 Å	[O/H] ₃ ^{NLTE} 7772 Å	[O/H] _{avg} ^{NLTE}	Instr.
HD 52919	4740 ± 49	4.25 ± 0.10	1.03 ± 0.09	-0.05 ± 0.06	18.1	0.06	-0.07	14.7	0.06	-0.05	10.8	0.06	-0.03	-0.05 ± 0.10	[3]
HD 53143	5462 ± 54	4.47 ± 0.07	1.08 ± 0.07	0.22 ± 0.06	66.7	0.24	-0.04	60.1	0.29	0.04	42.6	0.30	0.11	0.04 ± 0.11	[3]
HD 57095	4945 ± 54	4.45 ± 0.10	1.09 ± 0.08	-0.03 ± 0.06	32.8	0.25	0.08	-	-	-	24.0	0.37	0.24	0.16 ± 0.13	[3]
HD 64606	5351 ± 68	4.62 ± 0.07	0.92 ± 0.19	-0.71 ± 0.09	38.0	-0.14	-0.33	27.9	-0.21	-0.38	17.7	-0.29	-0.43	-0.38 ± 0.11	[3]
HD 67199	5136 ± 56	4.54 ± 0.08	0.84 ± 0.08	0.06 ± 0.06	44.7	0.28	0.08	40.0	0.33	0.14	28.9	0.28	0.13	0.12 ± 0.10	[3]
HD 100623	5246 ± 37	4.54 ± 0.05	1.00 ± 0.06	-0.38 ± 0.05	27.2	-0.29	-0.47	23.6	-0.24	-0.40	14.8	-0.33	-0.46	-0.44 ± 0.08	[3]
HD 102365	5667 ± 27	4.59 ± 0.02	1.05 ± 0.06	-0.27 ± 0.04	63.4	0.39	0.10	52.0	0.37	0.11	48.1	0.49	0.26	0.16 ± 0.11	[3]
HD 102438	5639 ± 51	4.60 ± 0.04	1.12 ± 0.10	-0.23 ± 0.06	54.1	-0.16	-0.42	47.4	-0.12	-0.36	40.0	-0.04	-0.25	-0.34 ± 0.12	[3]
HD 104304	5562 ± 50	4.37 ± 0.06	1.10 ± 0.06	0.27 ± 0.06	89.0	0.42	0.07	73.1	0.36	0.06	63.3	0.43	0.17	0.10 ± 0.10	[3]
HD 109200	5103 ± 46	4.47 ± 0.07	0.75 ± 0.07	-0.24 ± 0.05	37.0	0.12	-0.07	30.2	0.10	-0.07	24.6	0.17	0.03	-0.04 ± 0.10	[3]
HD 115617	5577 ± 33	4.34 ± 0.03	1.07 ± 0.04	0.01 ± 0.05	61.9	-0.01	-0.30	56.0	0.04	-0.23	40.1	-0.04	-0.25	-0.26 ± 0.07	[3]
HD 118972	5241 ± 66	4.43 ± 0.10	1.24 ± 0.08	-0.01 ± 0.08	49.0	0.17	-0.06	40.0	0.14	-0.06	31.0	0.15	-0.02	-0.05 ± 0.11	[3]
HD 125072	5001 ± 115	4.39 ± 0.21	1.21 ± 0.15	0.24 ± 0.11	-	-	-	33.0	0.34	0.18	24.0	0.29	0.16	0.17 ± 0.18	[3]
HD 128620	5844 ± 42	4.30 ± 0.04	1.18 ± 0.05	0.28 ± 0.06	98.0	0.24	-0.15	81.2	0.17	-0.16	70.7	0.23	-0.06	-0.12 ± 0.09	[3]
HD 128621	5199 ± 80	4.37 ± 0.12	1.05 ± 0.10	0.19 ± 0.09	43.6	0.14	-0.06	35.2	0.10	-0.08	27.2	0.10	-0.04	-0.06 ± 0.12	[3]
HD 135204	5332 ± 37	4.31 ± 0.04	0.84 ± 0.05	-0.11 ± 0.05	56.8	0.18	-0.09	50.2	0.21	-0.04	35.1	0.12	-0.07	-0.07 ± 0.07	[3]
HD 136352	5667 ± 43	4.39 ± 0.03	1.08 ± 0.09	-0.31 ± 0.06	75.0	0.07	-0.27	68.0	0.13	-0.18	46.6	0.00	-0.24	-0.23 ± 0.08	[3]
HD 140901	5645 ± 37	4.40 ± 0.04	1.14 ± 0.05	0.13 ± 0.05	70.6	0.07	-0.24	60.5	0.06	-0.21	47.5	0.05	-0.17	-0.20 ± 0.07	[3]
HD 144628	5071 ± 43	4.41 ± 0.06	0.82 ± 0.07	-0.36 ± 0.06	22.6	-0.24	-0.40	17.4	-0.28	-0.42	13.8	-0.21	-0.33	-0.38 ± 0.09	[3]
HD 146233	5786 ± 35	4.31 ± 0.03	1.18 ± 0.05	0.08 ± 0.05	82.2	0.07	-0.28	67.6	0.01	-0.29	58.5	0.08	-0.18	-0.25 ± 0.09	[3]
HD 149661	5290 ± 52	4.39 ± 0.07	1.11 ± 0.07	0.04 ± 0.06	46.7	0.07	-0.16	36.2	-0.01	-0.20	27.2	-0.02	-0.17	-0.18 ± 0.09	[3]
HD 150689	4867 ± 87	4.43 ± 0.16	1.12 ± 0.13	-0.08 ± 0.08	14.0	-0.28	-0.39	11.0	-0.29	-0.39	9.0	-0.20	-0.28	-0.35 ± 0.16	[3]
HD 152391	5521 ± 43	4.54 ± 0.05	1.29 ± 0.06	0.03 ± 0.05	55.0	-0.03	-0.28	44.2	-0.07	-0.29	33.4	-0.08	-0.25	-0.27 ± 0.08	[3]
HD 154088	5414 ± 60	4.28 ± 0.08	1.14 ± 0.07	0.33 ± 0.07	67.4	0.28	0.00	59.0	0.29	0.04	47.3	0.29	0.08	0.04 ± 0.10	[3]
HD 154577	4973 ± 55	4.73 ± 0.08	0.94 ± 0.12	-0.62 ± 0.07	20.0	-0.10	-0.23	14.4	-0.16	-0.27	9.1	-0.08	-0.17	-0.22 ± 0.12	[3]
HD 156274	5300 ± 32	4.41 ± 0.04	1.00 ± 0.05	-0.33 ± 0.05	43.0	-0.03	-0.26	27.9	-0.23	-0.41	27.0	-0.03	-0.20	-0.29 ± 0.13	[3]
HD 165185	5942 ± 85	4.53 ± 0.05	1.39 ± 0.16	0.02 ± 0.10	96.0	0.12	-0.27	82.1	0.10	-0.24	70.9	0.17	-0.13	-0.21 ± 0.12	[3]
HD 165499	5950 ± 45	4.31 ± 0.02	1.14 ± 0.08	0.01 ± 0.06	95.7	0.09	-0.32	79.4	0.03	-0.32	64.4	0.03	-0.26	-0.30 ± 0.08	[3]
HD 170493	4854 ± 120	4.49 ± 0.23	1.36 ± 0.20	0.15 ± 0.13	22.0	0.10	-0.03	19.1	0.14	0.03	12.4	0.05	-0.04	-0.01 ± 0.21	[3]
HD 170657	5115 ± 52	4.48 ± 0.08	1.13 ± 0.07	-0.22 ± 0.06	33.1	0.00	-0.18	24.7	-0.07	-0.23	20.7	0.02	-0.11	-0.17 ± 0.11	[3]
HD 172051	5634 ± 30	4.43 ± 0.03	1.06 ± 0.05	-0.20 ± 0.04	52.5	-0.22	-0.49	42.3	-0.25	-0.48	35.2	-0.18	-0.38	-0.45 ± 0.08	[3]
HD 177565	5664 ± 28	4.43 ± 0.02	1.02 ± 0.04	0.14 ± 0.04	68.4	0.03	-0.26	63.3	0.10	-0.18	50.6	0.11	-0.11	-0.18 ± 0.10	[3]
HD 192310	5069 ± 49	4.38 ± 0.19	0.79 ± 0.07	-0.01 ± 0.05	29.5	0.34	0.17	25.9	0.02	-0.13	21.6	-0.27	-0.40	-0.12 ± 0.31	[4]
HD 219449	4757 ± 102	2.71 ± 0.25	1.71 ± 0.09	0.05 ± 0.14	52.2	0.41	0.12	47.5	0.45	0.18	40.2	0.48	0.24	0.18 ± 0.32	[4]

The instruments used to obtain the spectra were: [1]UVES; [2]UES; [3]FEROS; [4]SARG; [5]CORALIE.